

Palestine Polytechnic University

College of Engineering



Design a Microstrip UHF RFID Tag  
Antenna for Metallic Object Application

By

Imad Talahmeh

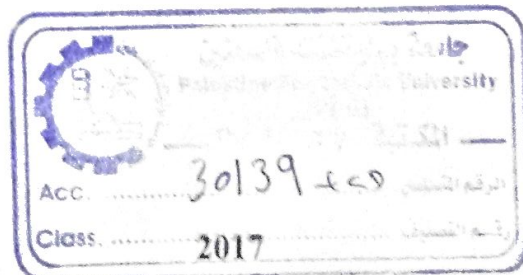
Jumana Alarameen

Supervisor: Dr. Arafat A.A. Shabaneh

Submitted to the College of Engineering

In Partial Fulfillment of the Requirements for the

Bachelor Degree in Communication & Electronic Engineering



Palestine Polytechnic University  
Collage of Engineering  
Electrical Engineering Department  
Hebron – Palestine

**Design a Microstrip UHF RFID Tag  
Antenna for Metallic Object Application**

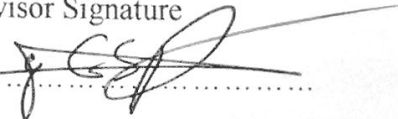
Project Team

Imad Talahmeh

Jumana Alarameen

Submitted to the Collage of Engineering  
In partial fulfillment of the requirements for the degree of  
Bachelor degree in Electronics and Communication Engineering.

Supervisor Signature

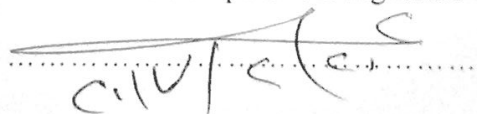


.....

Testing Committee Signature

.....

Chair of the Department Signature



.....

2017

## الاهداء

قال تعالى : اقرأ باسم ربك الذي خلق ﴿١﴾ خلق الإنسان من علق ﴿٢﴾ اقرأ وربك الأكرم ﴿٣﴾ الذي علم بالقلم ﴿٤﴾  
علم الإنسان ما لم يعلم ﴿٥﴾ " العلق

إذا كان الاهداء يعبر ولو بجزء من الوفاء

فالاهداء

الى

معلم البشرية ومنبع العلم نبينا محمد ( صلى الله عليه وسلم )

نهدي هذا العمل الي ارواح شهداء فلسطين

نهدي هذا العمل المتواضع الى الاب الذي لم يبخل علينا يوماً بشيء

والى الام التي زودتني بالحنان والمحبة

نقول لهم : انتم وهبتونا الحياة والأمل والنشأة على شغف الاطلاع والمعرفة

والى الاخوة و الاسرة جميعا

ثم الى كل من علمنا حرفاً أصبح سنا برفقه يضيء الطريق أمامي

## الشكر

نشكر الله العليّ القدير الذي أنعم علينا بنعمة العقل والدين. القائل في محكم التنزيل " وَفَوْقَ كُلِّ ذِي عِلْمٍ عَلِيمٌ "سورة يوسف آية 67... صدق الله العظيم.

وقال رسول الله (صلي الله عليه وسلم): " (من صنع إليكم معروفاً فكافنوه، فإن لم تجدوا ما تكافنونه به فادعوا له حتى تروا أنكم كافتموه) ..... " رواه أبو داوود.

ونثني ثناء حسنا على د. عرفات شبانه و د. فؤاد عرمان  
وأيضاً وفاءً وتقديراً وإعترافاً منا بالجميل نتقدم بجزيل الشكر لأولئك المخلصين الذين لم يألوا جهداً في  
مساعدتنا.

وأخيراً، نتقدم بجزيل الشكر إلي كل من مدوا لنا يد العون والمساعدة في إخراج هذه الدراسة علي أكمل وجه.

## Abstract

Deploying an RFID system on metallic object can present many challenges; the most challenging issue is that to have the antenna high gain, little reflection coefficient, and small size. The performance of RFID tag antennas can be improved using metamaterials. Some recent works have pointed out that metamaterial based antenna can have the same characteristics as large printed antenna.

The project represents the proposed split-ring resonator based UHF RFID tag antennas with regular ground plane and photonic bandgap ground plane for metallic application in the 917 MHz with high gain and appropriate reading range. the size of the tag antenna is  $84.5 \times 61.8 \times 1.57 \text{ mm}^3$ , which is placed on PTFE substrate with thickness 1.5 mm.

PBG structure is formed by placing any periodic shapes in the ground of the tag antenna, in this project periodic circles were placed in the ground of the tag antenna. After studying the PBG structure by trying different values of the diameters of the circles and the distance between these circles note that the effect be on the resonance frequencies without any improvement on the gain of the antenna, So trying periodic circles to form PBG did not help to improve the gain, may be different shapes rather than circles did that.

The gain of SRR based tag antenna with regular ground plane is  $-1.43 \text{ dB}$  when it placed on  $400 \times 400 \text{ mm}^2$ , but in the end of the project we note that the gain of the regular ground plane is always negative so to enhance this gain the parameters that constituent the antenna have been studied and we found that when the value of the parameter S reduced from 0.2 mm to 0.10 mm the gain of the antenna enhanced from  $-1.43 \text{ dB}$  to  $0.0563 \text{ dB}$  when the antenna placed on  $400 \times 400 \text{ mm}^2$ .

## ملخص المشروع

تطبيق نظام (RFID) على الاجسام المعدنية له عدة تحديات منها محاولة الحصول على قيمة عالية من ( antenna gain ) و قيمة منخفضة من ( antenna reflection coefficient ) بالاضافة الى المحافظة على حجم مناسب للانتيينا.

تم استخدام ( SRR ) في المشروع وهو احد انواع ( metamaterial ) المستخدمة في تصميم الانتيينات حيث انه بالاستناد الى البحوث السابقة فان عملية استخدام ( metamaterial ) في تصميم الانتيينا يساعد على تحسين ادائها و بالتالي الحصول على خصائص للانتيينا المصممة بحيث تكون قريبة لخصائص الانتيينا الكبيرة المستخدمة في تطبيقات اكبر.

هذا المشروع يقدم تصميم لنظام ( UHF RFID tag antenna ) و الذي تم تصميمه باستخدام ثلاثة طرق:

1. ( Regular Ground Plane ) و تم تطبيقه عند تردد ( 917 MHz ) حيث ان اكبر ( gain ) للانتيينا تم الحصول عليه باستخدام هذه الطريقة هو ( -1.43 dB ) و اكبر ( Read Range ) لهذه الانتيينا وصل الى ( 0.56 m ) و هذه النتائج تم الحصول عليها عند وضع التصميم على جسم معدني ابعاده (  $400 \times 400 \text{ mm}^2$  ).
2. ( Photonic Band Gap ) و تم عمله عن طريق وضع اشكال دائرة في ( ground ) للانتيينا و تم تجريب اقطار و مسافات مختلفة بين هذه الاشكال الدائرة و تم التوصل الى نتيجة ان ( PBG ) يعمل على تغيير ( operating frequency ) و في المقابل لا يوجد تحسين في ( gain ) و تم استنتاج ان اشخدام الاشكال الدائرية لتكوين ( PBG ) لا يحسن في ( gain ) ربما اشكال اخرى غير الاشكال الدائرية يمكنها تحسين ( gain ).
3. اثناء عمل هذا المشروع تم ملاحظة ان ( gain of the regular ground plane ) دائما ما تكون قيمته قليلة و لحل هذه المشكلة تم دراسة خصائص ال ( parameters ) المكونة للانتيينا المصممة و وجد انه عند تغير قيمة ( S ) من ( 0.2 mm ) الى ( 0.10 mm ) فان ( gain of regular ground plane ) تم تحسينه من ( -1.43 dB ) الى ( 0.0563 dB ) و بالتالي ( read range ) يكون اكبر.

حجم الانتيينا النهائي هو (  $84.5 \times 61.8 \times 1.57 \text{ mm}^3$  ) و تم اخذ قيمة ( gain ) باستخدام برنامج ( CST ) و تم التأكد من القيم باستخدام جهاز ( vector network analyzer ) و اخيرا تم استخدام ( RFID reader ) و الذي يحتوي على ( 20 dBm radiation power ) لتجربة الانتيينا .

## List of Figures

		<b>Page</b>
	An overview of basic RFID system	4
	UHF applications in (a) supply chain mangment and (b) retail item mangment	5
	Flowchart of the project	7
	RFID system block diagram	10
	Component of passive RFID system	13
	Component of active RFID system	14
	Fields regions around an antenna	21
	Definition of effective isotropic radiated power	23
	The equivalent circuit of an RFID tag	24
	Antenna impedance, chip impedance and read range versus frequency for typical RFID tag	25
	Two-port impedance model of an antenna and feed	31
	Schematic representation of a dipole antenna and its impedance	31
0	Photograph of the two-port measurment	32
1	Connections using the proposed two port jig to measure the impedance of a dipoles	32
2	Graphic illustration for snell's law with negative refractive index	35
	Flow chart of split ring resonator based tag antenna placed on metallic object	39
	An LC circuit	40
	Series and parallel LC resonant circuits	41
	Circular and square structures of split ring resonators	42
	Equivalent circuit model of SRR	43
	Equivalent circuit of another individual SRR	44
	Another antenna structure and it's principle of operation	46
	Equivalent circuit model for the circular SRR	46
	The proposed design	47

4.1	Geometry of the presented tag antenna, $S_x=61.8$ , $S_y=84.5$ , $D=1.57$ , $W=0.5$ , $S=0.2$ , $G=0.5$ , $G1=2$ , $L_a=60$ , $W_a=40.2$ (unit:mm)	52
4.2	Geometry of the presented tag antenna on CST program	52
4.3	Simulated reflection coefficient with $L_a=59$ (mm) and $W_a= 40.6$ (mm)	54
4.4	Simulated bandwidth with $L_a=59$ (mm) and $W_a= 40.6$ (mm)	54
4.5	(a) Semirigid coaxial cables (b) Open ended center conductor of semirigid coaxial cables (c) Examination the antenna using VNA	55
4.6	Simulated far-field radiation pattern at 917 MHz for designed tag antenna with regular ground plane mounted on $200 \times 200$ mm <sup>2</sup> metal plate.	55
4.7	Simulated far-field radiation pattern at 917 MHz for designed tag antenna with regular ground plane mounted on $400 \times 400$ mm <sup>2</sup> metal plate.	56
4.8	Simulated gain of the proposed design with regular ground plane placed on various metal plate sizes.	56
4.9	(a) The designed antenna (b) Backside of PBG design.	59
4.10	improved gain of regular ground plane , $S_y=61.8$ , $S_x=84.5$ , $D=1.57$ , $W=0.5$ , $S=0.1$ , $G=0.5$ , $G1=2$ , $L_a=59$ , $W_a=40.6$ (unit: mm)	61
4.11	Simulated reflection coefficient with $L_a= 59$ (mm), $W_a= 40.6$ (mm) and $S= 0.1$ (mm)	61
4.12	Simulated bandwidth with $L_a= 59$ (mm), $W_a= 40.6$ (mm) and $S= 0.1$ (mm)	62
4.13	Simulated far-field radiation pattern with $S = 0.10$ (mm) at 917 MHz for designed tag antenna with regular ground plane mounted on $200 \times 200$ mm <sup>2</sup> metal plate	62
4.14	Simulated far-field radiation pattern with $S = 0.10$ (mm) at 917 MHz for designed tag antenna with regular ground plane Mounted on $200 \times 200$ mm <sup>2</sup> metal plate	63



## List of Tables

Table		Page
2.1	The comparison between passive and active RFID system	15
2.2	The major difference between the kinds of RFID tags	16
2.3	RFID system characteristics	17
2.4	The classification of RFID classes according to some features	18
4.1	Simulated results of various values of $L_a$ and $W_a$ .	53
4.2	Theoretical maximum read range of the proposed design with regular ground plane.	57
4.3	Simulated results of various values of circular slot diameter and dimension between two circular slots when $L_a = 59$ (mm) and $W_a = 40.6$ (mm).	58
4.4	Theoretical maximum read range of the proposed design with photonic bandgap.	59
4.5	Simulated gain for the proposed antennas @ 917 MHz.	60
4.6	Simulated gain for the antenna @ 915 MHz when $S = 0.15$ mm.	60
4.7	Simulated gain for the antenna @ 917 MHz when $S = 0.10$ mm	63
4.8	Channel capacity of various data rate in the case of assuming noise with $S = 0.10$ mm	64
4.9	Simulated gain for the proposed antennas	64
4.10	Percent of reduction of the channel capacity when reducing $S$ from 0.2 mm to 0.1 mm	65
4.11	the received power for the proposed antennas @ 0.5 m	66

## List of Abbreviations

AIDC	Auto Identification and Data Capture
AUT	Antenna Under Test
AMC	Artificial Magnetic Conductor
ASIC	Application Specific Integrated Circuit
BW <sub>p</sub>	Percentage Bandwidth
BW <sub>r</sub>	Ratio Bandwidth
CSRRs	Complementary Split Ring Resonators
CST	Computer Simulation Technology
EAS	Electronic Article Surveillance
EIRP	Equivalent Isotropic Radiated Power
EM	Electromagnetic
EPC	Electronic Product Code
ERP	Effective Radiated Power
GHz	Gigahertz
HDPE	High Density Polyethylene
HF	High Frequency
HFSS	High Frequency Structure Simulator
HIS High	Impedance Surface
HPBW	Half-Power Beamwidths
IC	Integrated Circuit
ID	Identification
IFF	Identification of Friend or Foe
ISM	Industrial Scientific and Medical
SRD	Short Range Devices
IC	Integrated Circuits

EIRP		Equivalent Isotropic Radiated Power
ERP		Effective Radiated Power
PTC		Power Transmission Coefficient
PP		Polypropylene
VNA		Vector Network Analyzer
SMA		Sub-Miniature Version

## Table of Content

CHAPTER	Page
<b>1. INTRODUCTION</b>	
1.1 Research Motivation and Related Works	-2-
1.2 Research Motivation	-2-
1.3 Research Background	-3-
1.4 Research Objective	-5-
1.5 Research Methodology	-6-
1.6 Research Organization	-8-
<b>2. LITERATURE REVIEW</b>	
2.1 Introduction	-10-
2.2 Background of RFID	-10-
2.3 Brief History of RFID	-11-
2.4 RFID Tag Types and Classifications	-12-
2.4.1 RFID Tag Types Based on Power Supply	-12-
2.4.2 RFID Tag Operating Frequency	-16-
2.4.3 RFID Tag Classes	-18-
2.5 RFID Tag Antenna Design Considerations	-19-
2.5.1 Antenna Size and Shape	-19-
2.5.2 Bandwidth	-19-
2.5.3 Radiation Pattern	-20-
2.5.4 Directivity and Gain	-21-
2.5.5 Impedance Matching	-23-
2.5.6 Read Range	-26-
2.5.7 Data Rate and Channel capacity	-27-
2.5.8 Deformation	-29-
2.5.9 Fabrication Material and Process	-29-
2.5.10 Proximity to Objects	-29-
2.6 Impedance Measurement of RFID Tag Antenna	-30-
2.7 Properties of Metamaterial	-34-
2.7.1 Negative Refractive Index	-34-

2.7.2	Snell's Law with Negative Refractive Index	-35-
2.8	Application and Research Areas of Metamaterials	-36-
2.9	Summary	-36-
<b>3.</b>	<b>METHODOLOGY</b>	
3.1	Introduction	-38-
3.2	Design Components	-40-
3.2.1	Substrate	-40-
3.2.2	Modified Split Ring Resonator Based RFID Tag Antenna	-40-
3.2.2.1	Resonator	-40-
3.2.2.2	Resonance	-41-
3.2.2.3	Conceptual design of split ring resonator	-42-
3.2.3	Photonic Band Gap Structure	-48-
3.3	Summary	-49-
<b>4.</b>	<b>SPLIT RING RESONATOR UHF RFID TAG ANTENNAS</b>	
4.1	Introduction	-51-
4.2	SRR Based Antenna with Regular Ground Plane	-51-
4.2.1	Antenna Structure	-51-
4.2.2	Parametric Study	-53-
4.2.3	Simulation and Measurement Results	-54-
4.3	SRR Tag Antenna with PBG Ground Plane	-58-
4.3.1	Antenna Structure	-58-
4.4	Method to enhance the gain of the proposed antenna	-60-
4.5	Summary	-66-
<b>5.</b>	<b>SUMMARY AND DESIGN APPLICATION</b>	
5.1	Summary	-69-
5.2	Design Application	-69-
5.3	Future Work	-70-

# **CHAPTER ONE**

## **INTRODUCTION**

- 1.1 Research Motivation and Related Works**
- 1.2 Research Motivation**
- 1.3 Research Background**
- 1.4 Research Objective**
- 1.5 Research Methodology**
- 1.6 Research Organization**

# CHAPTER ONE

## INTRODUCTION

### 1.1 Research Motivation and Related Works

The key objective works of the present dissertation is dealing with presenting the simulations performance and the implementation fabrication of the radio frequency identification (RFID). Tag antenna can be applied in many applications such as placing the RFID tag antenna on a metallic object. While the challenges to reduce the antenna size and enhance the range of this antenna.

The novel contributions of this project are:

- Design and simulation of a miniaturized RFID tag antenna with regular ground plane and photonic band gap plane.
- Working and implementing fabrication for a metallic object application.
- Comparison the gain and the read range of the tag antenna between the simulated and the fabricated design.

### 1.2 Research Motivation

RFID technology is a wireless communication technology that used to uniquely identify tagged objects or people. It is an emerging technology and one of the most rapidly growing segments of today's automatic identification and data capture (AIDC) industry [1]. Whenever realize it or not, RFID is an integral part of our life. RFID is used for hundreds, if not thousands of applications such as inventory management, managing traffic, collecting tolls without stopping, gaining entrance to buildings, automating parking, security, mobile and healthcare. It is rapidly becoming a cost-effective technology and it is currently recognized as one as research area of priority. The development of RFID market is projected to increase from approximately 3 billion \$ in 2005 to 25 billion \$ in 2015. RFID allows items to have a unique identification code and have data stored on the chip about the product. In addition, it can read many items

simultaneously [2]. Product can get damaged during the transportation process; these errors are known as transaction errors. RFID could be implemented to reduce these transaction errors. RFID has the capability to improve business in all the ways just described as long as it is implemented correctly.

Recently, the applications of RFID passive systems operating in the ultra high frequency (UHF) band have experienced a progressive growth. UHF-RFID tags are usually designed to operate at a single frequency band. However, due to the different worldwide regulations, the UHF-RFID frequency bands have different locations in the spectrum and vary in the different world regions. Therefore, the design of UHF-RFID able to cover the whole regulated bands providing appropriate read performance becomes an important challenges. Another major problem which prevents a faster expansion of the UHF-RFID technology at present is found in potential application from high expectations arises: the retail item management. The problem is found in the difficulty of simultaneously offer the possibility of controlling items payment in the stores and inventory of elements present in the store .

### **1.3 Research Background**

The research worked presented in this thesis is in the area of RFID. RFID is an emerging technology used for object identification by means of radio waves. An RFID system consists of three major parts: a tag, associated with the object to be identified; a reader, used to extract the objects unique identifier from the tag; and an application system possibly in the form of a network. The tags and readers enable the automated identification of tagged objects, and the application system performs important tasks using this captured information.

Figure 1.1 shows the components of a basic RFID system. It tags are attached to objects that are to be identified. Each of the tags has a tiny chip (integrated circuit) that has memory and is capable of containing information.

The type of RFID tags considered in this research are passive (UHF) tags operating within the frequency (915-921 MHz) in the far field region with respect to the RFID reader antenna. For a passive tag, electromagnetic fields from a reader antenna are required to power up the tag. If the tag is successfully detected by the reader, information of the tag received by the reader will be passed on to application systems in a host computer (connected to the reader) for further data and information processing [3].



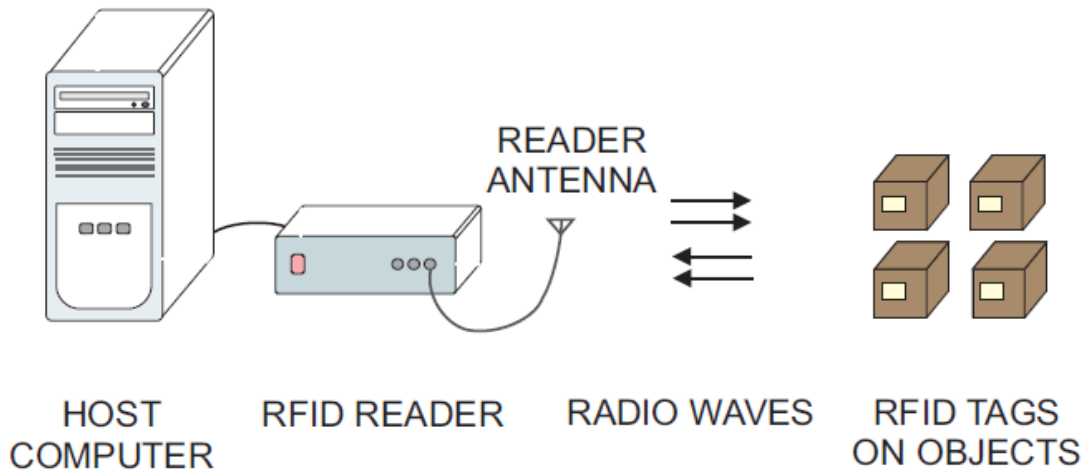


**Figure 1.1:** An overview of basic RFID system.

The major components of the system are reader (with reader antenna), tags (attached to objects) and a host computer (connected to the reader for data management). The host computer can be connected to the internet or a network consisting other computers for data sharing purposes.

There are many types of antennas used in the RFID, this project we concern with the Microstrip antenna for many reasons; these reasons are classified as follow as [4, 5]:

- Ease of manufacturing.
- Having low fabrication cost.
- It is an efficient radiation system.
- Having low volume.
- Conformal to multiple surfaces.
- Capable of dual and triple frequency operations.
- Can be easily integrated with microwave integrated circuits (MICs).

As mention early the RFID operate in the UHF usually of 433 MHz (active tags) and from 860 MHz to 960 MHz (Passive tags) there are significant difference between regulations in different countries around the world, such as United States, Europe, Japan and China.

UHF tags have a read range of up to 15 m approximately. Unlike low frequency (LF) and high frequency (HF) tags, all protocols in the UHF range have same type of anti collision capability, allowing multiple tags to be read simultaneously. The UHF tag antennas are mostly based on

dipole antenna and made of copper, aluminum or silver deposited on the substrate as shows in Figure 1.2.



**Figure 1.2:** UHF applications in (a) supply chain management and (b) retail item management.

Metallic objects are very common around us. Their presence is unavoidable and so to identify them, having the appropriate RFID tags suitable for operation on metallic surfaces is essential. Frequently, the tags must be small in size to allow identification at item level of individual small metallic objects.

An RFID system communicates by electromagnetic waves. When designing the RFID tag antenna mountable on metallic object, it is very important to understand the behavior of the electromagnetic field near metallic surface since the antenna parameters (the input impedance, gain, radiation pattern, and radiation efficiency) can be seriously affected by metallic platforms.

## 1.4 Research Objective

The main goal aim of this research program is to design and simulate UHF RFID system with regular ground plane and photonic band gap ground plane using a 3D full wave electromagnetic simulator (CST Microwave Studio, Version 2014) and fabricate the designed UHF RFID with photonic band gap plane simulation.

The objectives of the research includes the following aspects:

- To design a split-ring resonator-based RFID tag antenna with regular ground plane for metallic objects identification.

- To study the effect of integrating the PBG on the design performance of the tag antenna.
- To compare the performance between the simulated and the fabricated design tag antenna via measurements of their gain and read range.

## **1.5 Research Methodology**

Firstly, to achieve the objectives of this work, there is a need to study and understand the fundamentals of the SRR and how this type of material can be integrated with antennas ( the project implement the C- shape, in order to reduce the antenna size, increase the read range and to enhance the gain of the developed antenna ). Then, a computer simulation technology (CST) needs to be used to simulate the structures. Afterward, integrating PBG structure have been applied with tag antenna after it was successfully designed with regular ground plane for RFID application. Finally, measurements must be performs on the RFID tag antenna to validate the design method. The developed methodology for designing the RFID tag antennas is illustrated in the flow chart depicted in Figure 1.3.

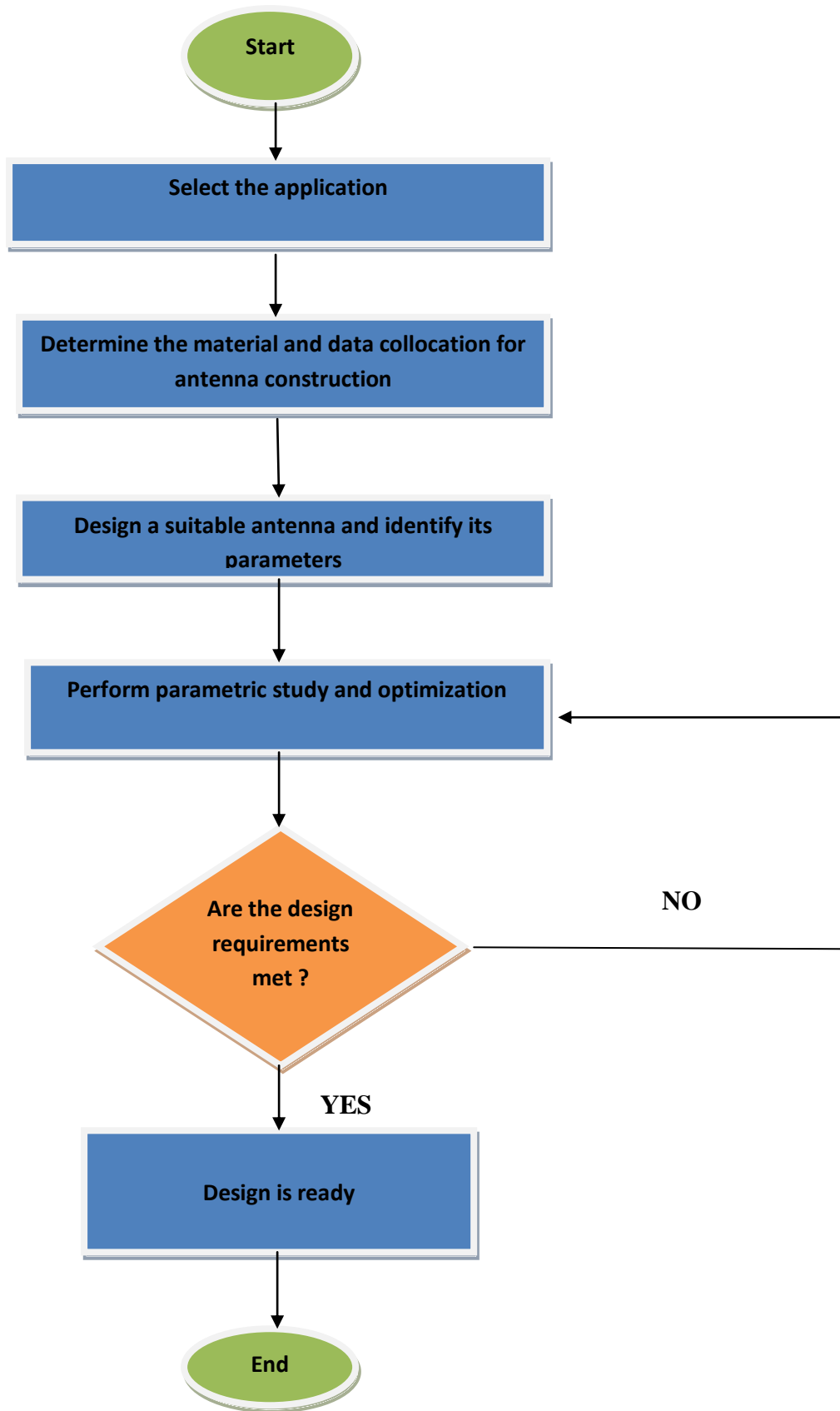


**Figure.1.3:** Flowchart of the project.

## **1.6 Research Organization**

This thesis compromise of five chapters. Which are summarizing as follows:

**Chapter one:** provides a background of research, and identifies the current reason, which motivated this research to design RFID tag antennas. It also introduces the goal objectives, methodology as well as the organization of project writing.

**Chapter two:** presents a literature review on RFID system and metamaterials. It first provides a background and history of RFID technology and some details about their classes and design considerations. Then detailing on salient electromagnetic features of the metamaterials as well as their recent applications. Finally, a summary of previous work.

**Chapter three:** describes the methodology used to design split ring resonator-based antenna structure in an attempt for achieving high gain. The performance of split-ring resonator based tag antennas are investigated in terms of achieving impedance matching and discuss the effects of integrating PBG structure on antenna performance. Parameters affecting resonance frequency included in this chapter. Methodology is finally summarized.

**Chapter four:** elaborates on a novel design of split-ring resonator-based RFID tag antennas. First tag antenna with regular ground plane and second tag antenna integrated with PBG structure to enhance the gain. Parametric study is also illustrated for various antenna parameters. The performance characteristics in terms of reflection coefficient, gain, resonance frequency and bandwidth. Finally, a summary on the chapter is reviewed at the end.

**Chapter five:** summarizing and concluding the entire project, followed by suggesting possible ideas for future work.

## **CHAPTER TWO**

### **LITERATURE REVIEW**

- 2.1 Introduction**
- 2.2 Background of RFID**
- 2.3 Brief History of RFID**
- 2.4 RFID Tag Types and Classifications**
  - 2.4.1 RFID Tag Types Based on Power Supply**
  - 2.4.2 RFID Tag Operating Frequency**
  - 2.4.3 RFID Tag Classes**
- 2.5 RFID Tag Antenna Design Considerations**
  - 2.5.1 Antenna Size and Shape**
  - 2.5.2 Bandwidth**
  - 2.5.3 Radiation Pattern**
  - 2.5.4 Directivity and Gain**
  - 2.5.5 Impedance Matching**
  - 2.5.6 Read Range**
  - 2.5.7 Data Rate and Channel Capacity**
  - 2.5.8 Deformation**
  - 2.5.9 Fabrication Material and Process**
  - 2.5.10 Proximity to Objects**
- 2.6 Impedance Measurement of RFID Tag Antenna**
- 2.7 Properties of Metamaterial**
  - 2.7.1 Negative Refractive Index**
  - 2.7.2 Snell's Law with Negative Index of Refraction**
- 2.8 Application and Research Areas of Metamaterials**
- 2.9 Summary**

# CHAPTER TWO

## LITERATURE REVIEW

### 2.1 Introduction

This chapter addresses for the background and the brief history of RFIDs. Then some details on RFID tag classification and challenges in their antenna design are presented. After that a brief review of the state of the antenna designs for RFID is provided. Lastly, summary and conclusions are given by the end of the chapter.

### 2.2 Background of RFID

A typical RFID system is composed of three different parts, as shown in Figure 2.1. The RFID tag (transponder), the reader (interrogator), the application software that is needed in order to act as an interface between the RFID system and its users. The tag carries the ID data, the reader extract the data from the tag; and the software helps this all happen more smoothly. RFID technology utilizes radio waves in order to transmit data back and forth between the reader and the tag. The reader transmits out radio waves, and in return it receives modulated return echoes; which are processed by the reader. After the tag modulates the electromagnetic wave and transmits the resulting data back to the reader, it is processed for things such as asset tracking, security surveillance and managerial purpose.

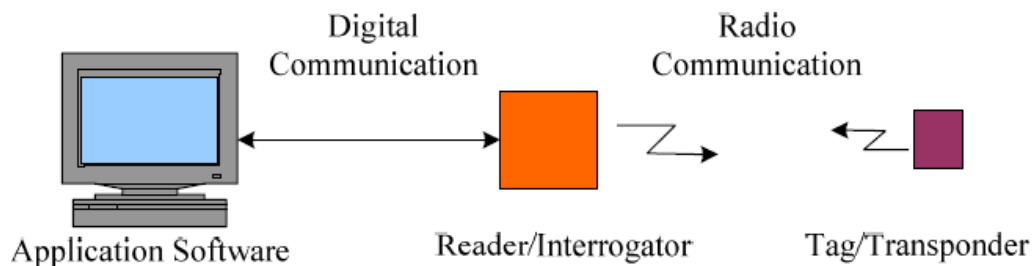


**Figure 2.1:** RFID System Block Diagram

## 2.3 Brief History of RFID

Although RFID only became known to many in recent years due to the widening of its applications, the concept of RFID has actually existed decades ago. It can be traced back to as early as a round the World War II era. Listed below, in chronological order are significant events that led up the RFID of today [6-8]:

- In 1935, Sir Robert Alexander Watson-Watt led to the development of an “Identify Friend or Foe (IFF) ” system using radar. The IFF system was used in World War II to detect and differentiate between friendly and enemy aircraft. Friendly aircraft would transmit a signal back upon receiving signal from a ground radar station for identification. This radar concept is very closely related to the RFID concept.
- In the 1960s, Electronic Article Surveillance (EAS) systems were developed and commercialized for merchandize anti-theft purposes. EAS tags are 1-bit tags that can be in either “on” or ”off” state. When attached merchandize, they can indicate whether an item of merchandize has been legitimately sold. A deactivated (“off” state) EAS tag can pass through EAS tag reader without triggering an alarm.
- In the 1970s, more development work on RFID started to take place. Scientists from Los Alamos scientific laboratory released their results on their research titled “Short-Range Radio-Telemetry for Electronic Identification using Modulated Backscatter”. Developments were aimed at applications such as animal and vehicle tracking.
- In the 1980s, full implementation of RFID systems for various applications took place. Due to the advancement complementary metal oxide-semiconductor (CMOS) integrated circuit technology, smaller RFID tags with more functionality were able to be produced. The RFID tags at that time were made of combination of (CMOS) circuits and discrete component.
- In the 1990s, further advancement of technology allowed RFID tags consisting a single (CMOS) integrated circuit and without discrete component to be produced.
- In 1999, an organization called the Auto ID-Center at Massachusetts Institute of technology was established. The organization introduced the vision and idea using RFID to track and identify every object in supply chain down to an item level. To allow this, the cost of the tag should be minimal. Hence, the concept of each tag



having a unique ID called the Electronic Product Code (EPC) stored in the RFID integrated circuit or chip of the tag was introduced. Instead of requiring a large memory to store huge amount of data related to an object, the tag chip is only required to have enough memory to store the EPC, which point to more information of a particular object stored elsewhere in the data base.

- In 2003, after much preliminary research and development to achieve its vision, the Auto-ID Center passed on its work and responsibilities to two newly founded organizations, the Auto-ID labs and EPC global. The purpose of the Auto-ID labs is to continue the technical research and development aspects of the RFID technology, while EPC global aims to develop RFID standards for seamless global deployment of RFID systems. At the same time, RFID related standards are also being developed by another organization called International Organization for Standardization.

## **2.4 RFID Tag Types and Classification**

### **2.4.1 RFID Tags Types Based on Power Supply**

There are three classifications of RFID Tags based on power supplies:

1. **Passive tags:** It is a simplest form in common use today, an RFID system consists of three elements, as shown in Figure 2.2 [9]. The RFID tag element consists of an antenna integrated with a microchip. The RFID reader antenna transmits an electromagnetic RF signal. This signal is received by the RFID tag via the tags antenna. The energy in the received signal provides the power to the tag that allows the microchip to operate. This is referred to as “passive” tag.

This data from the microchip is then added to an RF signal that is reflected by tag back to the reader through the reader antenna. This process is referred to as passive backscatter. The reader contains the electronics to receive this signal from tag, extract the RFID tags code from the signal, and return it to its digital form, and provide that returned code to a host computer.

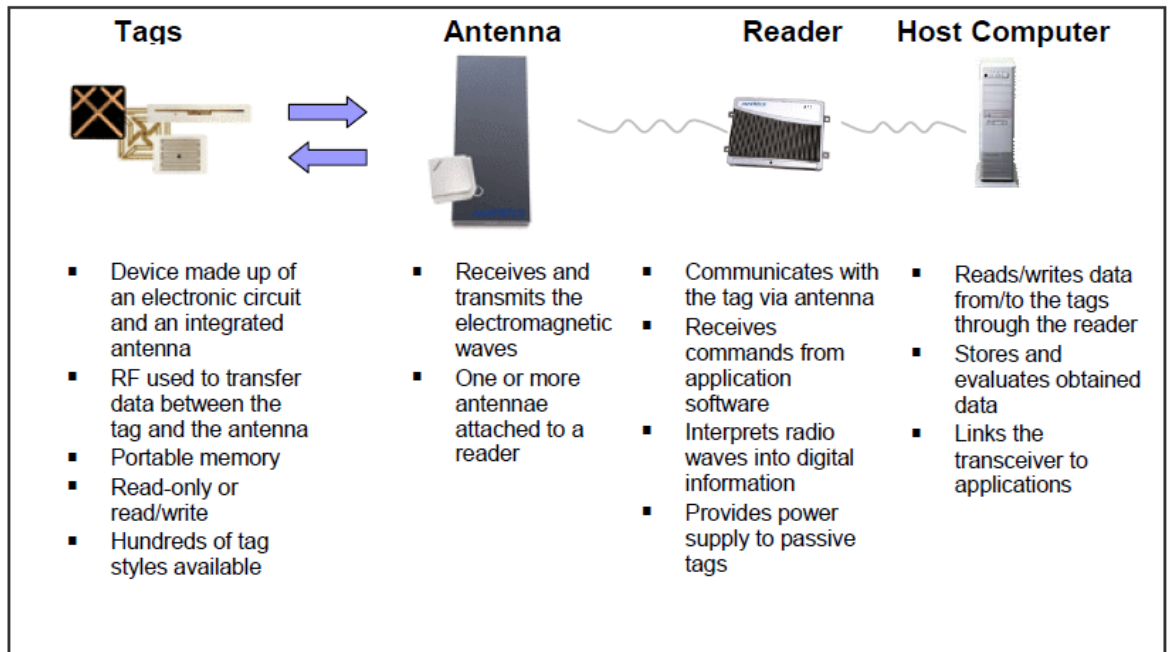


**Figure 2.2:** Component of passive RFID system.

Passive tag systems are reader talk first. The tags are mute until a signal is received from a reader. Also, one reader at a time can energize a passive tag; if more than one reader tries to light up a passive tag a collision known as “reader collision” occurs.

In terms of cost, passive RFID tags range from \$0.25 up to \$10.00 depending on functionality, packaging, and application. The price of passive RFID tags is highly dependent on the volume of tags ordered . Lower volumes will generally lead to much higher per tag prices.

In a common application of RFID technology today, RFID tag are combined into an adhesive label that can be applied to packaging for products in the consumer packaged goods supply chain.

2. Active tags: it is more advanced tags that also available. These tags may include small batteries. These “active” tags, as depicted in Figure 2.3[9], allow them to broadcast a stronger signal that can be received at greater distances than the “passive” tags powered only by the signal received from the reader/antenna system. A key differentiator between active and passive tags is the style of communications. An active tags talks first, since the tag is not depending on a reader to be energized, and because signal processing technology is so powerful, active tags can be read at

much greater ranges than passive tags. Active tags can also be used for positioning determining the XYZ location of tag through a process of triangulation.

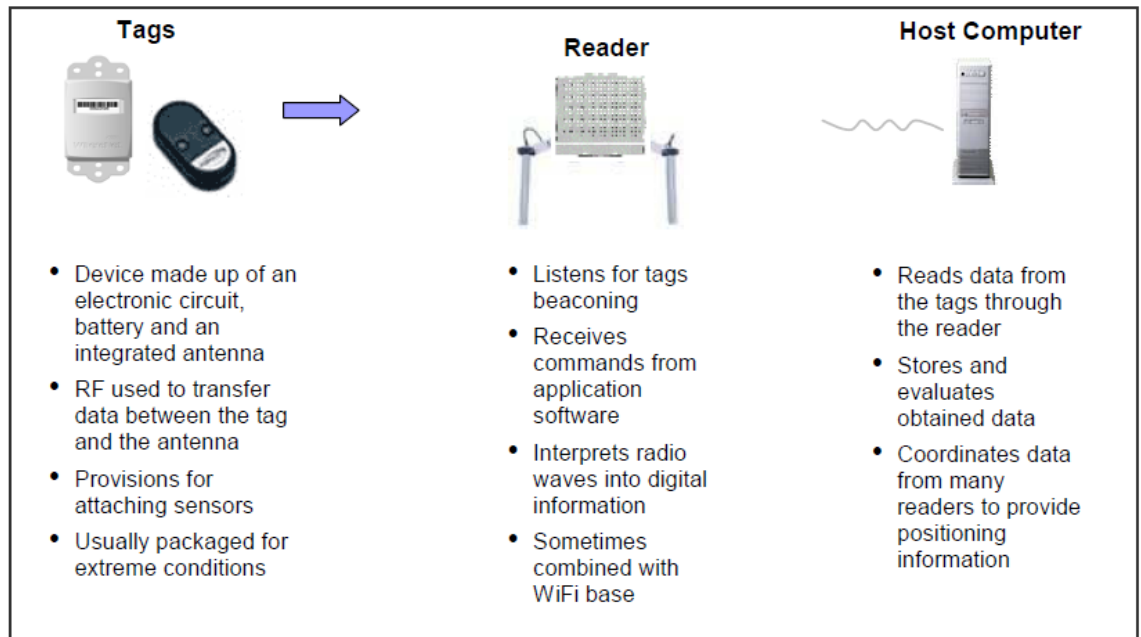


**Figure 2.3:** Components of active RFID system.

Since there is a communication channel involved, active tags can be integrated with sensor devices, such as temperature, location or motion sensor. These devices can take samples from the sensors, store them, and send them back to the reader along with the standard beacon signal. Table 2.1 shows the main difference between the active and passive RFID system.

**Table 2.1.:** The comparison between passive and active RFID system.

	Active RFID	Passive RFID
<b>Best Features</b>	<ul style="list-style-type: none"> <li>• Real-time location</li> <li>• Uses existing Wi-Fi network</li> <li>• Reusable tags with replaceable batteries</li> <li>• Site-wide visibility</li> </ul>	<ul style="list-style-type: none"> <li>• Low-cost tags</li> <li>• Small tag sizes and formats</li> <li>• Writable memory</li> <li>• No batteries required</li> </ul>
<b>Limiting Features</b>	<ul style="list-style-type: none"> <li>• Tag cost and size</li> <li>• Battery life – long-term storage</li> <li>• Insufficient Wi-Fi coverage</li> </ul>	<ul style="list-style-type: none"> <li>• Read range</li> <li>• “Last seen” knowledge</li> <li>• Chokepoint location restraints</li> </ul>
<b>Best Use Cases</b>	<ul style="list-style-type: none"> <li>• Large area coverage</li> <li>• High-value or high-impact assets</li> <li>• Cell-based manufacturing</li> <li>• Highly variable movement patterns</li> </ul>	<ul style="list-style-type: none"> <li>• High volume of assets</li> <li>• Lower costs assets</li> <li>• Continuous flow, narrow movement patterns</li> <li>• Supply chain operations</li> </ul>

3. Semi-active tags: these tags are akin to passive tags in that they are reader talk first. A battery is present through for one of two reasons. Either it is providing a boost for the tag, allowing it to be read and respond in difficult RF environments, or it is used to power a sensor. Such sensors can collect data even when the tag is read. This much slower read process than standard tag reading. The battery and sensor portions of semi-active tags can drive costs into \$5.00-\$10.00 range .

The difference between the previous three tags is classified in the Table 2.2.

**Table 2.2:** The major difference between the kinds of RFID tags.

Tags and Features	Passive Tag	Active Tag	Semi-Active Tag
Internal power source.	NO	Yes	Yes
Signal by backscattering the carrier wave from the reader	Yes	No	Yes
Response	Weaker	Stronger	Stronger
Size	Small	Big	Medium
Cost	Less expensive	More expensive	Less
Range	10 centimeters to few meters	Hundreds of meters	Hundreds of meters
Sensors	No	Yes	Yes

#### **2.4.2 RFID Tags Operating Frequencies**

RFID systems are designed to operate with low frequency (LF) up to Super high frequency (SHF). The communication between the tag antenna and the reader is determined by knowing the frequency operation band for the RFID systems. Identifying a vehicle and accessing parking lot are just a few of the wide range using of Low Frequency RFID [10]. Meanwhile, the few of primary implementation of high frequency systems are contact-less smart cards, credit cards, passports and access control systems. UHF RFID system can be used for various implementation from supply chain to inventory management to product tackling. The read rang of this system extends up to 10 meters which is considered a quite large. The unlicensed industrial scientific and medical (ISM) and short range devices (SRD) frequency bands that are used for RFID are illustrated in Table 2.3.

**Table 2.3:** RFID system characteristics.

Frequency Bands	Data & Speed	Read Range	Typical Usages	Strengths / Challenges
Low Frequency (LF): 125-134 KHz	Low read speed Small amounts of data	Very short inches	Access control Animal tagging Inventory control Car immobilizer	Low tag costs Small read range Small data amounts Low data transfer speed
High Frequency (HF): 13.553 - 13.567 MHz	Medium read speed Small to med amounts of data	Short to med: 1 to 3 feet	Smart cards Item or case Level tagging	Sufficient data amounts Most standards in place Less susceptible to interference
Ultra High Frequency (UHF): 433 MHz	Good data speed Medium to large amounts of data	Long range 50 – 300 Feet	Active tags Container seals Container tracking for DLA	Read speed and range Costs Potential interference with certain devices
Ultra High Frequency (UHF): 860-960 MHz	High read speed Small to med amounts of data	Medium: 2 to 10 feet	Pallet or case Level tagging SENTRI/MEXUS	Better read range High tag costs High data transfer speed More susceptible to interferences

### 2.4.3 RFID tags classes

The Auto ID center has classified the UHF RFID tags according to the way they operate. Table 2.4 shows these classifications. They are divided into 6 classes as stated below [11, 12]:

- Class 0: UHF read only programmed passive tag that used in order to communicate to the reader.s
- Class 1: a passive read only backscatter tag with one time field programmable.
- Class 2: a passive read write tags that can be written to any point in the supply chain.
- Class 3: a semi passive backscatter tag with read write memory.
- Class 4: read write active tags with integrated transmitters, can communicate with other tags or readers.
- Class 5: similar to class 4 tags but with additional functionality: can provide power to other tags and communicate with other devices than readers.

**Table 2.4:** The classification of RFID classes according to some features.

	Class 0	Class 1	Class 2	Class 3	Class 4	Class 5
Description	Factory programmed read-only tag	User-programmed read-only tag	Read-write passive tag	Semi-passive read-write tag	Active read-write tag	Active autonomous read-write tag
Passive/active	Passive	Passive	Passive	Semi-passive	Active	Active
Read/write	Read-only	Read-only	Read-write	Read-write	Read-write	Read-write
Transmission reliability	Low	Low	Low	High	High	High
Battery	No	No	No	Lithium/manganese	Lithium/manganese	Various types possible
Life span	High	High	Short	High	High	High
Communication range	Low	Low	High	Mid	High	High
Wireless mesh network	No	No	No	No	No	Yes

## **2.5 RFID Tag Antenna Design Considerations**

### **2.5.1 Antenna Size and Shape**

Small tag antenna size is better and more reliable to use in our life because it can be embedded and attached to objects like cardboard boxes, airline baggage strips, and the alike. Increasing antenna gain requires larger tags. Evidently, tag size and gain should be compromised.

The antenna size depends on the length and width of the metamaterial SRR and on the wavelength of the operating frequency. Typically, antenna sizes are approximately one-fourth wavelengths of the lowest operating frequency .

Antenna complex impedance depends on the size and shape of the antenna. Among different possible antenna shapes, a C-shape was chosen considering that we can use it to miniaturize the size of the tag antenna. Hence, adjusting the impedance by changing the shape is more advisable.

To attain a conjugate match an inductive antenna requires the resistive-capacitive behavior of the ASIC's impedance. Due to the limitation of size the matching network impedance must be embedded within the antenna for impedance modification. The changes in various antenna parameters regarding length and area might perform amendments of inductive-resistive characteristics.

### **2.5.2 Bandwidth**

Bandwidth is one of the basic characteristics of the UHF RFID technology. The bandwidth can be considered to be the range of frequencies, on either side of a center frequency, where the antenna characteristics (such as input impedance, radiation pattern, beam width, side lobe level, beam direction, radiation efficiency) are within an acceptable value of those at the center frequency.

The bandwidth could be related to the antenna band. In fact, this is the case of small antennas where a fundamental limit is related to its bandwidth, and its efficiency. Antenna bandwidth can be defined in various ways.



- Ratio bandwidth ( $BW_r$ ) [13, 14]: is defined in Equation 2.1 as:

$$BW_r = \frac{f_u}{f_l} \quad (2.1)$$

Where  $f_u$  and  $f_l$  are the upper and lower frequency of the band, respectively.

- Percentage bandwidth ( $WB_p$ ): it is related on the ratio bandwidth as in Equation 2.2 [13, 14]:

$$WB_p = 100 \left( \frac{f_u - f_l}{f_c} \right) = 200 \left( \frac{f_u - f_l}{f_u + f_l} \right) \% \quad (2.2)$$

Where  $f_c = \frac{f_u + f_l}{2}$ ;  $f_c$  is the center frequency

### 2.5.3 Radiation Pattern

The radiation pattern refers to the directional dependence of the strength of the radio waves from antenna. there are two types of radiation patterns in each antenna which are: E-plane and H-plane.

Energy of antenna is not radiated equally in all directions. The radiation power pattern is the power density variations along a constant radius. An accurate measurement of the radiation pattern is only possible if the matching loss between antenna and chip is kept constant.

The antennas field regions are classified as the following [13, 14].

- a) Reactive near field region: the region immediately surrounding the antenna where the reactive field (stored energy ) is dominant.

- b) Near field (Fresnel) region: the region between the refractive near field and the far field where the field distribution is dependent on the distance from the antenna.
- c) Far field (Fraunhofer) region: the region farthest away from the antenna where the field distribution is independent of the distance from the antenna.

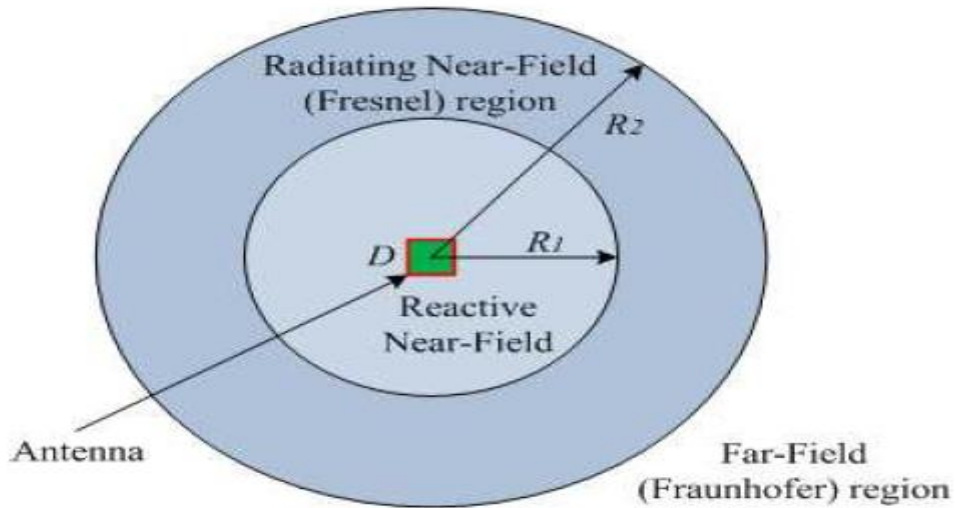


**Figure 2.4:** Fields regions around an antenna [13, 14].

The variation in distance from the reactive near field to the far field, cause changes in antenna’s amplitude and phase patterns.

### 2.5.4 Directivity and Gain

The directive gain is defined as the ratio of radiation intensity due to the test antenna to the isotropic antenna. As demonstrated in Equation 2.3, the directivity of a non isotropic source is equivalent to the ratio of its radiation intensity in a given direction [13]:

$$D = \frac{U}{U_i} = \frac{4\pi U}{P_r} \tag{2.3}$$

Where the directivity of the antenna is represented by  $D$ ;  $U$  represents the radiation intensity of the antenna;  $U_i$  represents the radiation intensity of the isotropic antenna; and  $P_r$  is the total power radiated in watts.

Meanwhile, gain, is a key performance number which combines the antenna directivity and the electrical efficiency. It defined as the ratio of the power produced by the antenna from a far field source to the power produced by an isotropic antenna.

An isotropic antenna radiates the same intensity of power in all direction, while a directive antenna radiates greater power in specific directions. Even though the antenna gain is measures the efficiency and the directional capabilities of an antenna. The directivity is a measurement in which only focuses to the property of antenna directionality. Particularly; the directivity of an antenna is always larger than that of its gain[13, 14], As shown in Equation 2.4:

$$G = \frac{A_{eff}}{\lambda^2 / 4\pi} = e_{cd} \frac{4\pi A_{phys}}{\lambda^2} = e_{cd} D \quad (2.4)$$

$$e_{cd} = \frac{A_{eff}}{A_{phys}} \quad (2.5)$$

Where  $e_{cd}$  the radiation efficiency factor of the antenna,  $A_{eff}$  is tha antenna aperture,  $A_{phys}$  is the physical aperture,  $D$  is the directivity, and  $G$  is the gain.

In national UHF regulations, radiated power is defined with different terms in the different countries. The two most common terms are EIRP and ERP.

EIRP (Equivalent Isotropic Radiated Power) mainly used in the US. Figure 2.5 shows how a directive antenna related to an isotropic antenna.

ERP (Effective Radiated Power) mainly used in Europe. Equation 2.5 shows the relationship between EIRP and the ERP [13, 14]:

$$EIRP (dB) = ERP (dB) + 2.15 \quad (2.6)$$

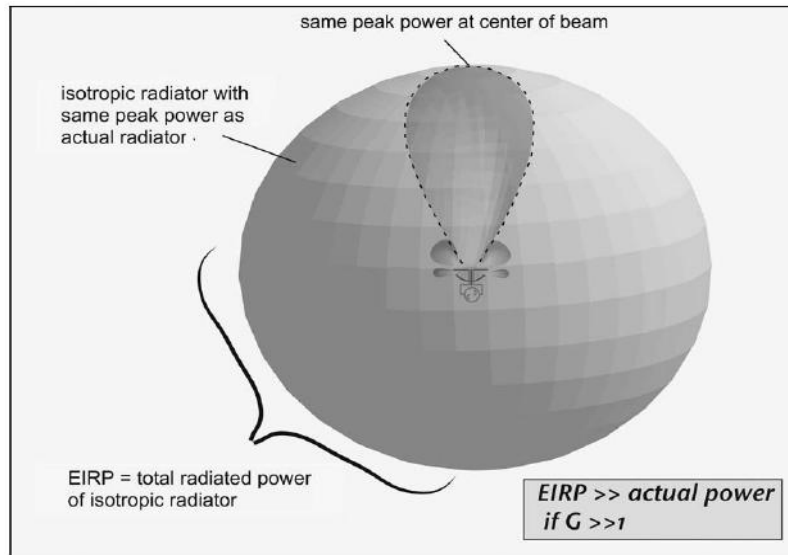


**Figure 2.5:** Definition of effective isotropic radiated power.

### 2.5.5 Impedance Matching

The goal of the tag antenna designer is to design an antenna that could increase the maximum detection range which is one of the performance characteristics of RFID system. A proper impedance matching between the antenna and the chip directly affects the performance characteristics of RFID system.

An RFID tag consists of a chip and an antenna. Depending on the match and mismatch between the chip and antenna impedance, power is absorbed or reflected by the tag. Thus to realize modulated backscattering the chip changes its input impedance to reach reflection of the RF power received from the reader. This is achieved by with a shunt transistor that is implemented in the tag chip.

The matching of tag antenna and chip strongly influence the communication performance between reader and tag. Since the input impedance of a chip cannot be chosen arbitrary due to technology limits, the antenna has to be designed to match the chips impedance. It is found that for a given tag chip; there exists two distinct optimum antenna impedances.

One maximizes the power available for the chip's internal circuitry this means power optimization of the forward link, and one maximizes the signal that is radiated towards the reader this means power optimization of the return link.

In RFID tags, there is usually a direct connection between the antenna and the chip, as demonstrated in Figure 2.7, where  $Z_a = R_a + jX_a$  is the complex antenna impedance and  $Z_c = R_c + jX_c$  is the complex chip (load) impedance.

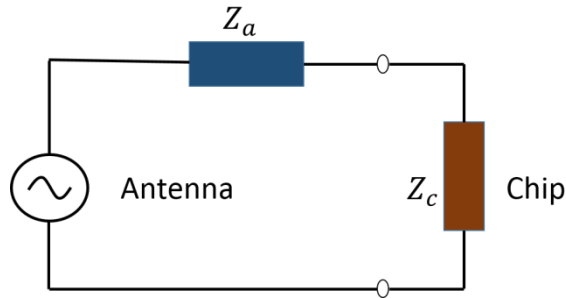


**Figure 2.6:** The Equivalent Circuit of an RFID Tag.

Frequency and input power vary depending on the different values of the complex impedance of the tag chip because it considers as a nonlinear load. The threshold is defined as a minimum voltage required starting the tag chip. The details of the chip's RF front end and the energy consumed by the specific chip [15] gauge the dependence the input impedance on the input power. The chip's parasitic and packaging effects identify the dependence of the impedance on the frequency.

The variation of the chip's impedance with power and frequency may be affected the performance of the tag. Attaining an excellent conjugate between an antenna and a tag chip is minimizing the power in need for the chip function in order to enhance the read range of the tag. Whenever the tag is in a proximity to the reader, the tag continuously operates because of the higher power incident on the tag.

the amount of power ( $P_c$ ) which the chip can absorb from the antenna is exhibited in Equation 2.6 [16]:

$$P_c = P_a \tau \tag{2.7}$$

Where  $P_a$  is the antenna's maximum power and  $\tau$  is the Power Transmission Coefficient (PTC).

Equation 2.7 illustrates the power transmission coefficient ( $\tau$ ) [17] :

$$\tau = \frac{4R_c R_a}{|Z_a + Z_c|^2}, \quad 0 \leq \tau \leq 1 \quad (2.8)$$

The power transmission coefficient ( $\tau$ ) is used to define the degree of impedance matching between IC chip and antenna.

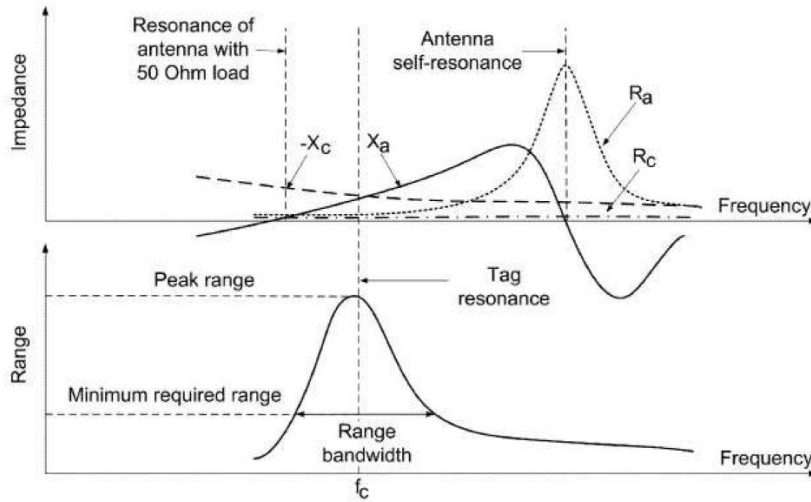


**Figure 2.7:** Antenna Impedance, Chip Impedance and Range versus Frequency for a Typical RFID Tag [16].

Figure 2.7 shows the behavior of the antenna and the chip impedance and the read range as a function of frequency for a regular RFID tag, the tag resonance is at the peak range ( $f_c$ ). Generally, the frequency of the best impedance matching between IC chip and antenna defines as tag resonance which is identified by  $\tau$  (Equation 2.8) with the frequency dependence dominated.

The antenna self-resonance and the resonant frequency of a 50 Ohm loaded antenna are not the same as tag resonance.

The power wave reflection coefficient ( $S_{11}$ ) is a parameter that describes how much of an electromagnetic wave is reflected by an impedance mismatch in a transmission medium, which exhibited [18] in Equation 2.9:

$$S_{11} = \frac{Z_a - Z_c^*}{Z_a + Z_c^*} \quad (2.9)$$

Reducing the power reflection coefficient  $|S_{11}|^2$  as in Equation 2.9 is recommended [19] to attain the most suitable match between the antenna and the IC chip:

$$|S_{11}|^2 = \left| \frac{Z_a - Z_c^*}{Z_a + Z_c^*} \right|^2 \quad (2.10)$$

The power reflection coefficient  $|S_{11}|^2$  is the complement of the power transmission coefficient  $\tau$  ( $|S_{11}|^2 = 1 - \tau$ ) and provides what fraction of the maximum power available from the generator is not delivered to the load.

### 2.5.6 Read Range

Read range is one of the most important performance parameters of RFID tags. One of the limitations of read range is maximum distance at which the tag receives enough power to be turned on and scatter back. The other one is the maximum distance where the scattered signal can still be detected by the reader. In general, the read range is determined by the former distance since the reader sensitivity is high enough[19].

Read range for an RFID tag is affected by many factors, including:

- Passive or Active RFID tag antenna.
- RFID frequency: LF, HF or UHF.
- Surrounding materials.
- Type of tag.
- Type of reader.
- Time to read.
- Number of tags being read.
- Density of tags.

The Friis free-space transmission formula is used to compute the power collected by an RFID antenna as shown in Equation 2.10 [13] :

$$P_r = \frac{P_t G_t G_r \lambda^2}{(4\pi r)^2} \quad (2.11)$$

Where  $P_t$  represents the transmitted power of the reader,  $G_t$  is the antenna gain of the reader,  $G_r$  is the received gain by tag antenna,  $\lambda$  is the wavelength, and  $r$  is the distance between the reader and the tag antenna.

The tag range bandwidth definition is the frequency band in which an acceptable minimum read range is offered by the tag over that band. The maximum possible read range  $r$  if the tag is perfectly matched to the chip is given in the bellow Equation [13]:

$$r_{max} = \frac{\lambda}{4\pi} \sqrt{\frac{P_t G_t G_r \tau}{P_{th}}} \quad (2.12)$$

Where  $P_{th}$  is the minimum threshold power required to turn on the chip.

When the antenna is perfectly matched to the chip ( $\tau = 1$ ), the maximum read range is possible as given in Equation 2.12:

$$r = \frac{\lambda}{4\pi} \sqrt{\frac{P_t G_t G_r}{P_{th}}} \quad (2.13)$$

### 2.5.7 Data Rate and Channel Capacity

The data transfer rate is the amount of the digital data that is moved from one place to another in a given time. Also it can be viewed as the speed of travel of a given amount of data from one place to another. In general, the greater the bandwidth of a given path, the higher the data transfer rate. The physical layer of the RFID system uses ASK / PSK backscatter, the minimum standard data rate for the system is 64 Kbps.



Channel capacity is the maximum rate at which the data can be transmitted over a given communication path or channel, and it is divided into two types:

1. Nyquist capacity formula

For an ideal transmission channel of bandwidth  $W$ , with no noise.

The maximum bit rate in this case is:

$$C = 2W \log_2 M \quad (2.14)$$

Where  $C$  is the channel capacity in bit/sec,  $W$  is the system bandwidth in Hertz and  $M$  is the signal level.

2. Shannon capacity formula

Very famous result due to Shannon (1948) states that the maximum possible transmission rate or capacity of a link of bandwidth  $W$  (Hz) and received signal to noise ratio SNR is

$$C = W \log_2(1 + SNR) \quad (2.15)$$

In actual systems the communication quality for data transmission is stated as a probability of bit error or bit error rate. Theoretically, we can get up to  $C$  (bps) with zero error rate. In practice, the actual bit error rate is always non zero. For any particular type of transmission technique over a bandwidth  $W$ , the bit error rate is a function of the SNR.

To obtain the quantity related to the SNR, the following equation is used.

$$\frac{S}{N} = \left( \frac{E_b}{N_o} \right) \left( \frac{R}{W} \right) \quad (2.16)$$

Where  $S$  is the signal power,  $N$  is the noise power,  $E_b$  is the energy per bit,  $N_o$  is the noise with power density,  $R$  is the bit rate and  $W$  is the bandwidth in hertz.

$S/N$  represent to SNR.

### **2.5.8 Deformation**

RFID tag antennas are usually designed for flat surface. Recently, modern RFID tag antennas were printed on low cost substrate. So, attaching these tag antennas to non-flat surfaces could highly affected the radiation properties causing deformation.

In fact, the antenna resonates at a different frequency because of impedance mismatch and de-tuning, which caused by the distortion of the geometry of an antenna.

### **2.5.9 Fabrication Material and Process**

To design a printed antenna there is a need to carefully know the two requirements that the design need : a substrate like polytetrafluoroethylene PTFE and a material with high conductivity as copper.

The substrate has three main parameters which are permittivity ( $\epsilon_r$ ), loss tangent ( $\tan \delta$ ), and the thickness. The effective wavelength is reduced with the use of any dielectric constant substrate. Furthermore, the resonance frequency will be lower and narrow bandwidth. The operating bandwidth will increase and the radiation power will reduce when the loss tangent of the substrate is high, but using high thickness substrates can avoid these effects.

### **2.5.10 Proximity to Objects**

Increasing the radiation resistance of the tag antenna is caused by proximity to conductive leading object to inefficient power transfer. For a specific object, a tag antenna can be designed or tuned to achieve optimum performance.

Objects with high loss dielectric constants, such as water and plastic is an object with high loss dielectric constant leading to tag detuning and radiation efficiency redaction.

## 2.6 Impedance Measurement of RFID Tag Antenna

In comparison with other RFID technologies which use LF and HF band, UHF RFID offers three advantages: data rate is higher, reading range is longer and material cost is lower. To achieve maximum power transfer, conjugate matching is compulsory between tag antenna impedance and tag chip impedance disregarding the different antenna designs .

Antenna simulation software is the most popular tool for antenna design such as high frequency structure simulation (HFSS), computer simulation technology (CST), there is an empirical process to design RFID system, i.e. the first step is identifying the specific design requirements before using the simulation for antenna design. Next, fabricated the prototype, then verification the simulation results with measurements.

The most important thing in the measurement of RFID tag antenna designs is the accuracy. UHF RFID is mostly used a symmetrical dipole and the loop antenna structures . These antennas with virtual ground are fed by a differential input signals. By using a conventional single-ended, two-port vector network analyzer (VNA), identifying the input impedance of the antenna would not be accurately obtained.

To measure the input impedance of balanced antenna different methods were proposed, which is the most common RFID antenna configuration. By utilizing a balun or imaging method, the impedance of a balanced antenna can be extracted. However, the size of the ground plane and the characteristic are the most important things which accuracy depends on. The use of measured S-parameter is proposed as alternative methods to measure the input impedance by connecting Microstrip lines or coaxial cables as test fixtures [20, 21].

Figure 2.9 shows the model proposed by the palmer for the impedance. The differential and common mode excitation voltages are represented by  $V_d$  and  $V_c$  respectively. Antenna feed terminals are nodes A and B.  $Z_a, Z_b$  and  $Z_c$  represent the antenna impedances where typically,  $Z_a = Z_b$  and are positioned between nodes A and B (antenna terminals) and ground, while  $Z_c$  is the impedance between A and B.

$Z_{common} = (Z_a // Z_b)$  is the common mode impedance and  $Z_{diff} = Z_c // (Z_a + Z_b)$  is the differential mode input impedance.

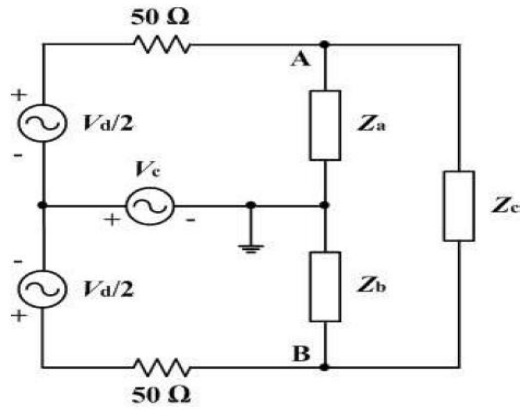


**Figure 2.8:** Two-Port Impedance Model of an Antenna and Feed [22].

The load or symmetrical antenna is considered as a device with three terminals when it is simulated. In case of a dipole antenna, one arm is connected to node A and the other to node B. The ground of the transmission lines is the same as the ground feeding the dipole arms. This two port dipole network connection is shown in Figure 2.9. The network analyzer ports connect to each arm of the dipole in the shown order. The dipole impedances are also shown in a schematic manner.

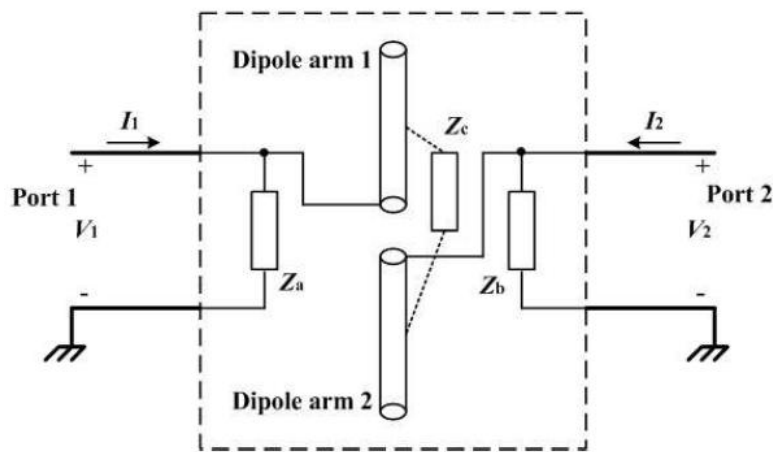


**Figure 2.9:** Schematic Representation of a Dipole Antenna and its Impedances.

A photograph of the proposed jig to measure balances loads is presented by a photograph in Figure 2.10, while dipole measurement by the jig and exhibiting how to connected it is shown in Figure 2.11. VNA is evident where each port is connected through test cables to one of the semi-rigid cables, respectively. The two semi-rigid cables are soldered together on their outer

conductors, while their inner conductors are partially extended to place the feeding points closer to the terminals of the antenna under test.

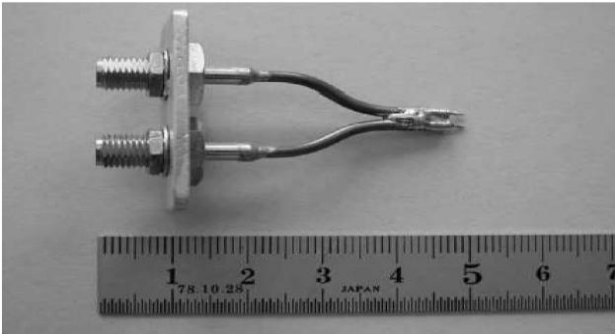


**Figure 2.10:** Photograph of the Two-Port Measurement jig [23].

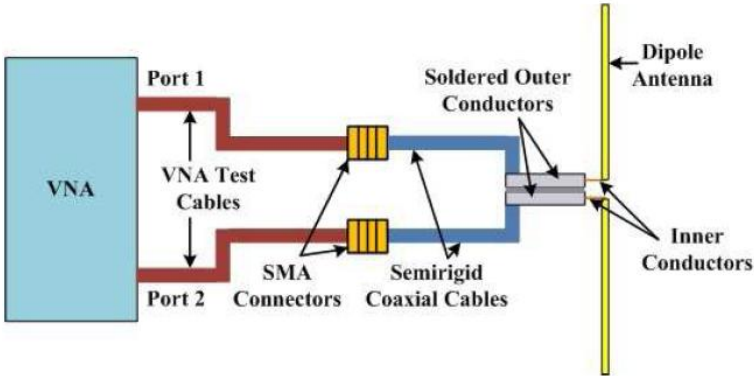


**Figure 2.11:** Connections Using the Proposed Two-Port Jig to Measure the Impedance of a Dipoles [22].

The measurement of the antenna is achieved by five steps:

1. The VNA is calibrated at the sub-miniature version A (SMA) connectors by making use of the supplied standards of the manufacturer.
2. From the short circuit measurement the two semi rigid cables parameters are determined.
3. The antenna is placed and its two-port S-parameters are measured.
4. By deem bedding the effect of the semi-rigid coaxial cables from the S-parameters at the SMA connectors, the antenna S-parameters are obtained.
5. The antenna impedances are derived from the S-parameters.

Characterization of the semi-rigid cables of the jig is performed during step 2 of the measurement. To simplify, each cable is considered as a transmission line with attenuation  $\alpha$  and phase delay  $\beta$ . For the measurement of these values, to obtain their complex input reflection coefficients a short to ground is set at the end of the semi-rigid cables.  $\beta l$  is obtained from this phase measurement which is double the electrical length of the cable and also a  $180^\circ$  phase reversal because of the short placed at both ends, while  $\alpha l$ , the line attenuation, is obtained when the measured magnitude (in nepers) of the reflection coefficient is divided by 2.

ABCD-parameters with  $\alpha$  and  $\beta$  [24] are obtained by Equation 2.13:

$$\begin{bmatrix} \text{Cosh}(\alpha + j\beta)l & Z_0 \sinh(\alpha + j\beta)l \\ \frac{1}{Z_0} \sinh(\alpha + j\beta)l & \text{Cosh}(\alpha + j\beta)l \end{bmatrix} \quad (2.17)$$

Where  $Z_0$  is normalized to 1.

The antenna impedances,  $Z_{diff}$  and  $Z_{common}$ , are desirable at this point since the parameters,  $S_{11}$ ,  $S_{21}$ ,  $S_{12}$  and  $S_{22}$  are already known. The following steps were done to come up with these impedances: First of all, the S-parameters were used to get the ABCD-parameters of the full measurement.

Next, an isolation of the antenna's ABCD-parameters is performed. This was performed by eliminating the effect of the semi-rigid cables from the full measurement, which required the pre and post-multiplication of the ABCD-parameters of the full measurement with the inverse ABCD-parameters of the two semi-rigid cables. Then, the obtained antenna ABCD-parameters are converted into Y-parameters. Thus, by making use of the Y-parameters, the impedances  $Z_a, Z_b$  and  $Z_c$  are obtained. Lastly, Equations 2.14 and 2.15 shows the impedances  $Z_{diff}$  and  $Z_{common}$  respectively:

$$Z_{diff} = \frac{Z_c(Z_a + Z_b)}{Z_a + Z_b + Z_c} \quad (2.18)$$

$$Z_{common} = \frac{Z_a Z_b}{Z_a + Z_b} \quad (2.19)$$

Where  $Z_a, Z_b$  and  $Z_c$  are the impedance as shown in Figure 2.8.

## 2.7 Properties of Metamaterial

### 2.7.1 Negative Refractive Index

A negative index of refraction is the name for an electromagnetic phenomenon where light rays are refracted at an interface in the reverse sense to that normally expected. The negative index metamaterial have negative  $\epsilon_r$ ,  $\mu_r$ , and  $n$ . Mathematically, this can be proven as follows:

$$n = -\sqrt{\epsilon_r \times \mu_r} \quad (2.20)$$

When  $\epsilon_r < 0$  and  $\mu_r < 0$ , Equation 2.16 can be rewritten as:

$$n = \sqrt{(-1) \times \epsilon_r \times (-1) \times \mu_r} \quad (2.21)$$

$$n = \sqrt{(-1)} \times \sqrt{(-1)} \times \sqrt{\epsilon_r \times \mu_r} \quad (2.22)$$

$$n = j \times j \times \sqrt{\epsilon_r \times \mu_r} \quad (2.23)$$

Where the complex number  $j = \sqrt{(-1)}$ .

Then,

$$n = -\sqrt{\epsilon_r \times \mu_r} \quad (2.24)$$

Equation 2.24 indicates that a negative radical in refractive index is obtained when  $\epsilon_r$  and  $\mu_r$  have negative values simultaneously.

### 2.7.2 Snell's Law with Negative Index of Refraction

Snell's law of refraction is a formula used to describe the relationship between the angles of incidence and refraction, and it is described as:

$$n_1 \sin \theta_1 = n_2 \sin \theta_2 \quad (2.25)$$

Where  $n_1$  is the refractive index of medium 1,  $n_2$  is the refractive index of medium 2,  $\theta_1$  is the incident angle, and  $\theta_2$  is the refraction angle.

According to Snell's law, if medium 1 and medium 2 are conventional materials with  $n_1 > 0$  and  $n_2 > 0$ , respectively, the refracted ray will be bent in a positive angle ( $\theta_2 > 0$ ) away from the line normal to interface NN'. But if the refractive index of medium 2 is less than zero ( $n_2 < 0$ ), the refracted ray will be bent in an unusual way in a negative angle ( $\theta_2 < 0$ ) away from NN' as shown in Figure 2.12. For this reason, left-handed materials are also called negative index materials.

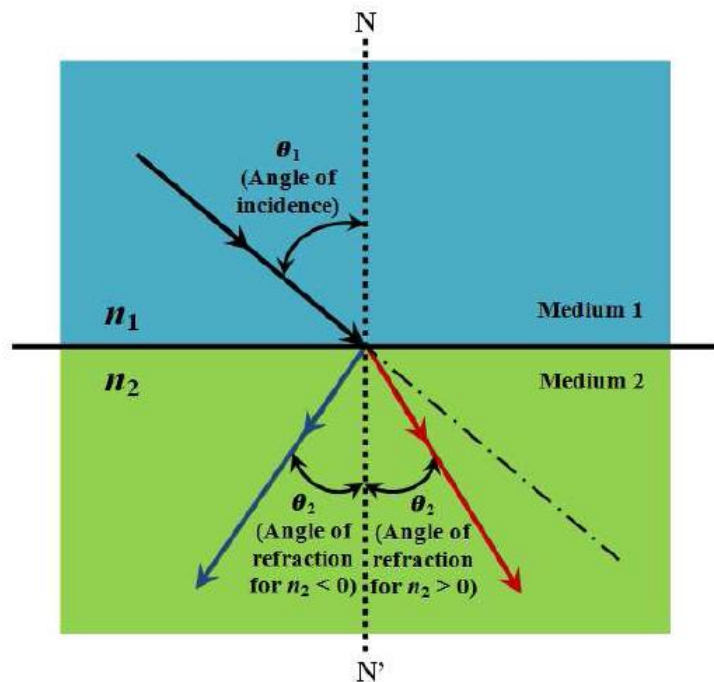


**Figure 2.12:** Graphic Illustration for Snell's Law with Negative Refractive Index.



## 2.8 Application and Research Areas of Metamaterials

The defense industry and medical equipments like microwave imaging to detect cancers or tumors used metamaterial antennas. The power radiation, directivity, and bandwidth efficiency performance characteristics are improved when Incorporation of metamaterial with antennas, especially for small spaces or platforms. Besides that, improving filter performance in terms of compactness, low insertion loss, high return loss, high selectivity, and good out of band rejection at low costs which are highly demanded characteristics for progress of the current, as well as future, wireless communication system applications . There is growing interest in perfect lens with resolution beyond the diffraction limits [25].

## 2.9 Summary

the previous sections of this chapter talks about the design of RFID tag antenna for metallic objects within the UHF (860-960) MHz range, history, basic classifications, properties. The most important performance parameters for tag antenna design are the size and the reading range. According to Friis free-space transmission formula (Equation 2.13). the read range depends mainly on the antenna gain ( $G_r$ ) and the threshold power ( $P_{th}$ ) of the use RFID chip. The antenna size is the tradeoff with its gain and bandwidth.

# **CHAPTER THREE**

## **METHODOLOGY**

### **3.1 Introduction**

### **3.2 Design Components**

#### **3.2.1 Substrate**

#### **3.2.2 Modified Spilt Ring Resonator Based RFID Tag Antenna**

##### **3.2.2.1 Resonator**

##### **3.2.2.2 Resonance**

##### **3.2.2.3 Conceptual design of split ring resonator**

#### **3.2.3 Photonic Band Gap Structure**

### **3.3 Summary**

## **CHAPTER THREE**

### **METHODOLOGY**

#### **3.1 Introduction**

This chapter presents the methodology of designing tag antennas for metallic application. Firstly, this chapter shows the designs substrate, which preferred over other materials for several reasons. Secondly, exhibiting information that's help in modified SRR based RFID tag antenna. In addition, how to achieve a good conjugate between the antenna and the IC chip through using inductively coupled feed to feed the split ring resonators will it is exhibits a flexible technique to match the input impedance of antenna and IC chip. Furthermore, it displays the photonic band gap structures (PBG). Finally, the summary introduced at the end of this Chapter.

Figure 3.1 show the methodology of SRR based UHF RFID antennas with regular ground plane and PBG ground plane.

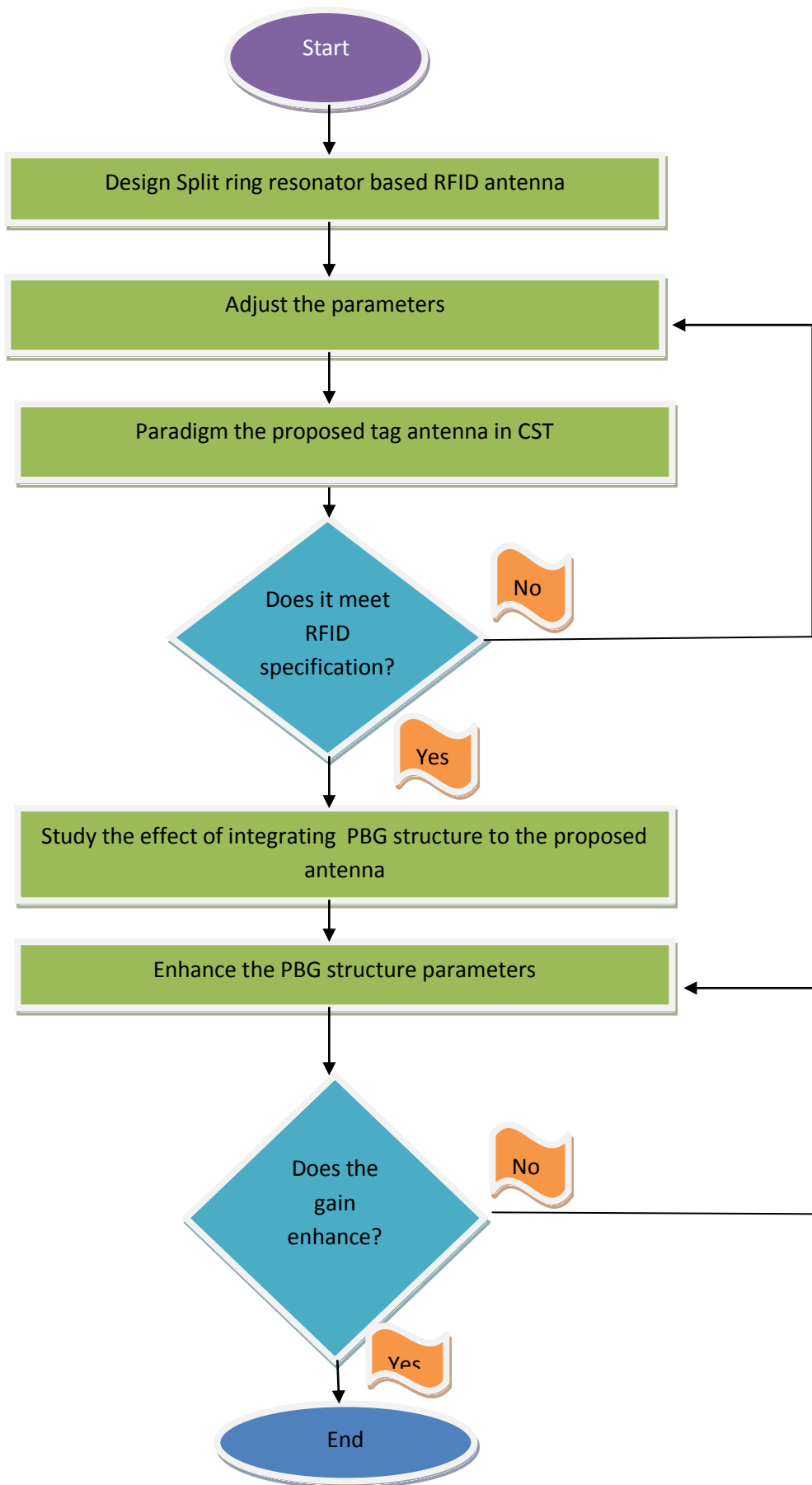


**Figure 3.1:** Flow chart of split-ring resonator-based tag antenna placed on metallic object.

## 3.2 Design Components

### 3.2.1 Substrate

The most sensitive factor in antenna's performance is the dielectric constant of the substrate material, as well as  $\epsilon_r$ .

Several substrate materials are available; their dielectric constant has a wide range, from 1.17 up to 25. They also are available with loss tangents from 0.0001 to 0.004 [26, 27].

PTFE which is abbreviation for Polytetrafluoroethylene is the most used materials; that is placed as a separator between the antenna and the reference ground plane for the Microstrip antenna. PTFE substrate with dielectric constant 2.55 can attenuate more than 95% of the parasitic current from the reference ground plane and the antenna will maintain approximately always the maximum power transfer with the IC chip, avoiding power losses and increasing the efficiency of the RFID tag. The most important reasons that preferred using PTFE over other materials are: the ease of processing, dimensional stability, little electrical losses.

### 3.2.2 Modified Split Ring Resonator Based RFID Tag Antenna

#### 3.2.2.1 Resonator

A resonator is a device that oscillates naturally with greater amplitude at certain frequencies than at other frequencies.

An LC circuit can be represented as a resonant circuit, it consists of a capacitor and an inductor. When the inductor and the capacitor are connected together, the resultant circuit can function as an electrical resonator.

LC circuit can be used in many circuits such as oscillators, filters, tuners, radars, and mixers. The major objective of the LC circuits are either generating signals at a particular frequency, or picking out a signal at a particular frequency from a complex signal.

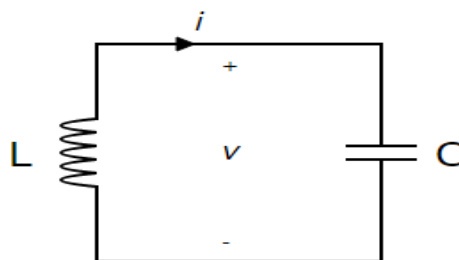


**Figure 3.2.** An LC circuit

### 3.2.2.2 Resonance

Resonance is a phenomenon in which a vibrating system drives another system to oscillate with greater amplitude at a specific frequency. It occurs when capacitive equals inductive reactance in magnitude, and the frequency at which two reactance hold for specific circuits is named the resonance frequency of the circuit. LC circuits has a resonance frequency which written as:

$$f_r = \frac{1}{4\pi\sqrt{LC}} \quad (3.1)$$

Where  $f_r$  is the resonance frequency, L is the inductance in (henrys), and C is the capacitance in (farads).

LC circuits can be either series or parallel circuits, for the series resonant circuits, as the inductance rises the capacitance decreases; the opposite is true in the case of parallel resonant circuits.

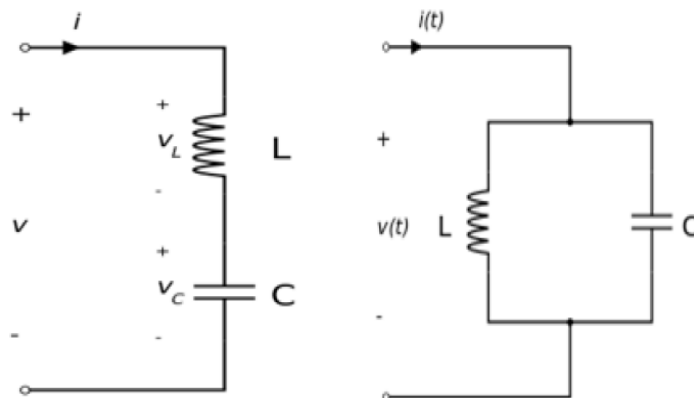


**Figure 3.3.** Series and parallel LC resonant circuits.

### 3.2.2.3 Conceptual design of split ring resonator

The split ring resonator consists of two metallic rings; either circular, square or carved on dielectric substrates and they always have gaps on opposite sides. The SRR is a composite material that has received growing interest in recent years for its use to construct metamaterials. The size of the SRR's is much less than the wavelength of an incident electromagnetic wave. As a result, the effective medium principle is applicable while working with split ring resonators. Large values of capacitance are produced in the resonators due to the small gaps between the rings; the capacitance is inversely proportional to the resonance frequency of the rings.



**Figure 3.4.** circular and square structures of split ring resonators

The SRR operates because while current can not flow around any one ring due to the split separation, the capacitance between two rings allow the flow of displacement current. SRR's can be modeled as LC circuits in the areas where the inductance arises from the rings.

The design configuration of SRR which fabricated on RF4 printed circuit to enhance the performance of RFID tag antennas. Some recent works have pointed out that metamaterial based antennas[28] can have the same characteristics as large printed antennas. The purpose of SRR is to produce magnetic response in various types of metamaterial up to 200 terahertz. These media create the necessary strong magnetic coupling to an applied electromagnetic field, not otherwise available in conventional materials.

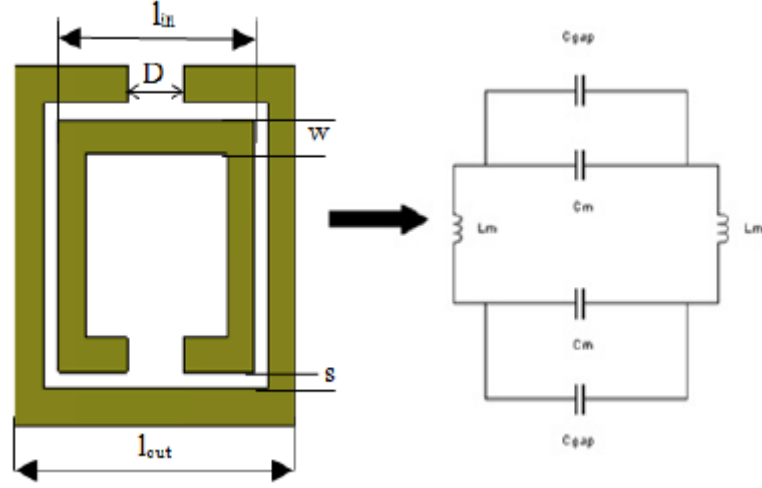


**Figure 3.5.** Equivalent circuit model of SRR [29].

Researches have shown that an individual SRR can realize the electromagnetic performances of SRR's array. The individual SRR may be modeled by an equivalent electrical circuit as shown in figure 3.5. The previous circuit can be modeled by an LC circuit. The presence of a magnetic field  $H$  perpendicular the plane supporting the two splits ring, allows the creation of the  $C_{gap}$  capacity at the opening of each ring to allow the ring to conduct and gives rise to current flow. The current flowing through the rings will enable it to act as an inductor and the dielectric gap between the rings will lead to mutual capacitance. In addition, each ring resembles a solenoid that can be represented by an inductance  $L_m$ . The space between the two rings will be modeled by capacity  $C_m$ .

To facilitate understanding of the previous circuit, these equations [29] can be helpful.

$$L_m = \frac{\mu_0 S}{W} (L_{out} + L_{in}) \quad (3.2)$$

$$C_{gap} = \frac{\epsilon_0 \epsilon_r t_c}{D} \quad (3.3)$$

$$C_m = \frac{A \epsilon_0 \epsilon_r W (2 L_{out} + 2 L_{in} - D)}{2 S} \quad (3.4)$$

$$f_o = \frac{1}{2\pi \sqrt{L_m (C_m + C_{gap})}} \approx \frac{1}{2\pi \sqrt{L_m C_m}} \quad (3.5)$$



Where ( $L_m$ ) is the inductance of each ring, ( $C_{gap}$ ) is the capacity of the slot ring, ( $C_m$ ) is the capacity created between two rings, and ( $f_o$ ) is the resonance frequency. Also with ( $L_{out}$ ) and ( $L_{in}$ ) are the length of the outer and inner ring, ( $W$ ) is the width of the strip of metal ring, ( $S$ ) is the space between the two rings, ( $D$ ) is the gap, and ( $A$ ) is the balance constant.

The author of the previous design [29] found that when the value of the gap ( $D$ ) decreases the resonance frequency will also decrease. He also concluded that the value of the width of the ring ( $W$ ) proportionally affects the values of the resonance frequency, the return loss, and the bandwidth of frequencies.

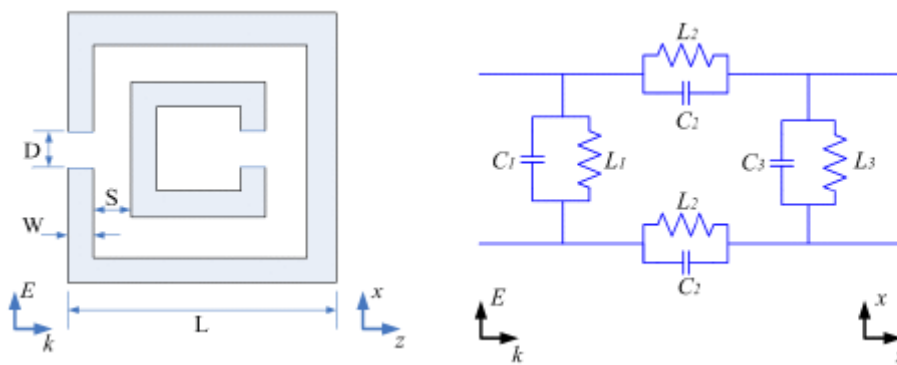


**Figure 3.6.** Equivalent circuit of another individual SRR [30].

The geometry of an individual SRR can be represented in another form as Figure 3.6. It functions as current sheets while an incident plane wave magnetic field  $H$  is penetrating through it. There are two splits in the outer ring and the inner ring of SRR. The equivalent circuit of this geometry is also represented in Figure 3.6 which has several inductors called ( $L1, L2, L2, L3$ ) and several capacitors called ( $C1, C2, C2, C3$ ).

$L1$  and  $L3$  represent the self inductors by an integrated sheet, while  $L2$  produced by one integrated outer and inner current sheet. The total capacitances of SRR consist of two parts, one part is the coupling capacitance between the outer and the inner rings, while the other part is produced the electric charges accumulate at the two splits. The coupling capacitance can be estimated using the following equations [30]:

$$C_C = [ 0.06 + 3.5 \times 10^{-5} (r_{out} + r_{in}) ] \quad (3.6)$$

$$C_O = \frac{1}{4} [ 0.06 + 3.5 \times 10^{-5} (r_{out} + r_{in}) ] \quad (3.7)$$

Where ( $C_C$ ) is the total coupling capacitance of SRR, and ( $C_O$ ) is the coupling capacitance for each side of the SRR. ( $r_{out}$ ) and ( $r_{in}$ ) represent the radius of the outer and the inner circumference of the SRR. Because of intense electromagnetic, there is a difficulty of estimating the capacitances at the outer and inner splits, so they are estimated by corrected the parallel plane capacitance formula as the following [30]:

$$C_{inner \ split} = \frac{3 \epsilon_0 S}{D} \quad (3.8)$$

$$C_{outer \ split} = \frac{25 \epsilon_0 S}{D} \quad (3.9)$$

The distributed capacitance  $C_1$ ,  $C_2$ , and  $C_3$  can be determined by using the following approaches [30]:

$$C_1 = C_O + C_{outer \ split} \quad (3.10)$$

$$C_2 = C_O \quad (3.11)$$

$$C_3 = C_O + C_{inner \ split} \quad (3.12)$$

The authors of the previous design [30] employ the equivalent circuit model to predict the resonance frequencies of the SRR. According to the geometry parameters  $L, W, S, t$  and  $D$  the author apply the formulas to determine the distributed elements  $L_1, L_2, L_3, C_1, C_2$ , and  $C_3$ . They found that equivalent circuit model can simultaneously predict three resonant frequency points with high precision, which is extremely important for SRR based metamaterials.

The equivalent circuit model can be advantageous to probe the root of the negative permeability, especially helpful for engineers to analyze SRR based metamaterials over multiple frequency bands.

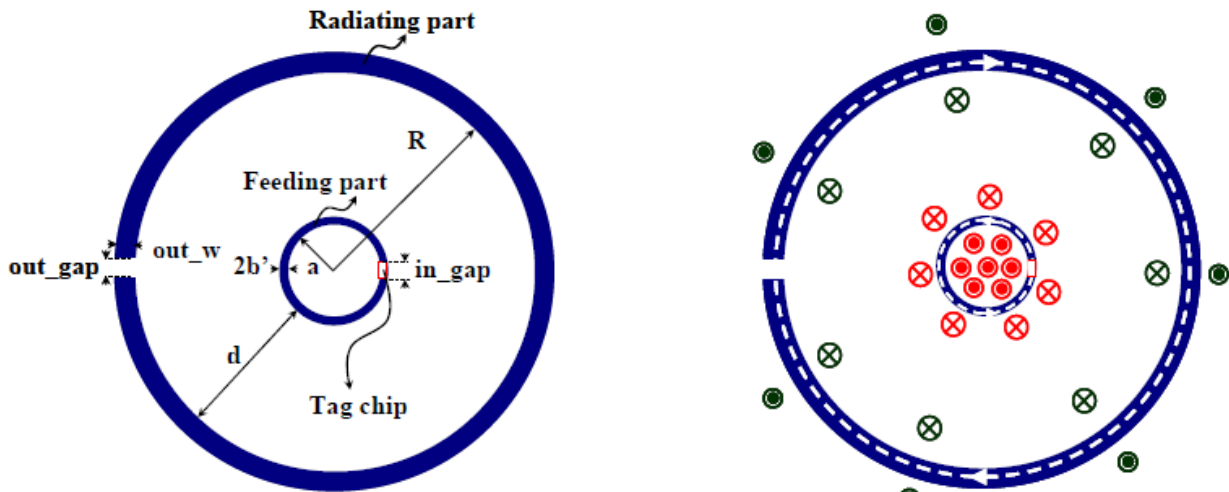


Figure 3.7. Another antenna structure and it's principle of operation [31].

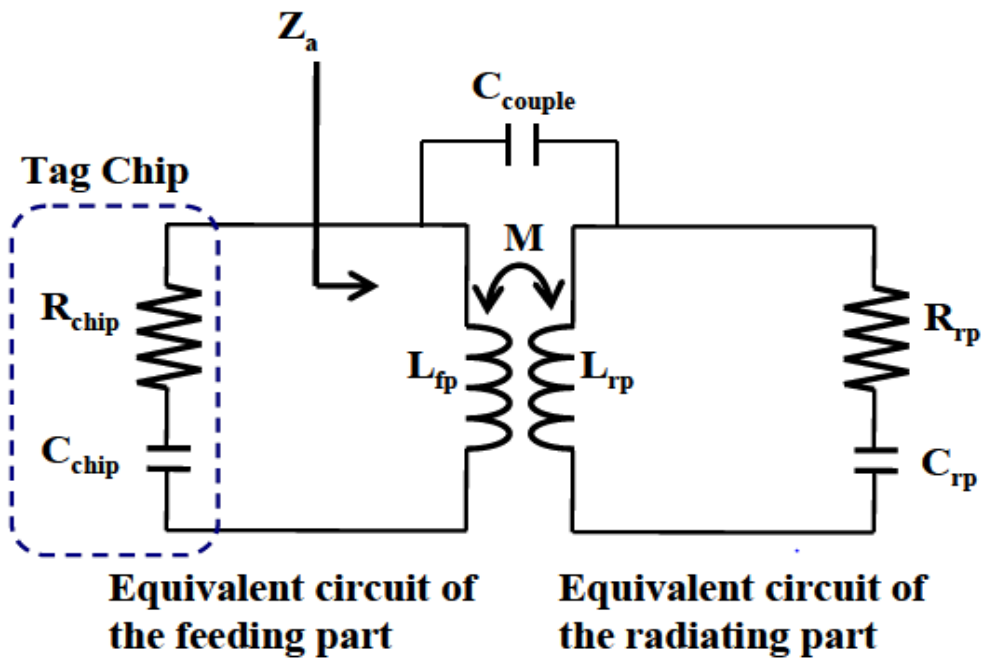
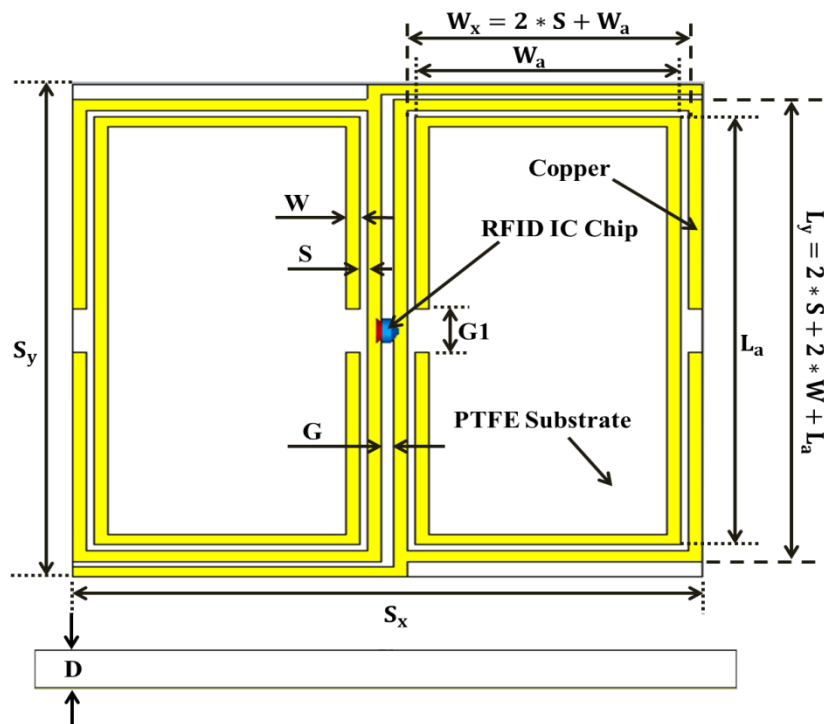


Figure 3.8. Equivalent circuit model for the circular SRR [31].

Figure 3.7 represents UHF RFID tag antenna which has a SRR as radiating part to reduce antenna size, also by using inductively coupled feeding method we can size obtain wide bandwidth and utilize simple matching technique to directly attach to a tag chip. The current flows on the feeding part because the feeding part is much smaller than the wavelength of

UHF frequency ranges. The current which flows in clockwise directions also is induced on the radiating part. It is the source to radiate in the freespace.

The capacitance ( $C_{couple}$ ) in the equivalent circuit between the feeding part and the radiating part is negligible because the distance between two parts is much larger than the area of feeding and radiating part. Also (M) represents the mutual inductance between the two parts,  $R_{rp}$  and  $Q_{rp}$  are the radiation resistance and quality factor of the radiating part at the resonance frequency, respectively.  $L_{fp}$  is the self inductance of the feeding part.



**Figure 3.9.** The proposed design [32]

The paper [32] presents a novel square SRR based UHF RFID tag antenna for metallic objects which is represented in figure 3.9, the choosing of this antenna is because the ease of fabrication, and it is an enhancement of the above SRR. It consists of two symmetrical C shaped resonators with outer strip lines to feed the SRR structures through implementing an inductively coupled feed approach placed on the top surface of PTFE substrate.

The input impedance of tag antenna can be obtained by selecting a proper length and width of SRR, which leads to attain an excellent conjugate match between antenna and IC chip.

A typical antenna occupies a major space of the entire design, so choosing for metamaterial based antenna will theoretically reduce the size and enhance the performance. The reasons of choosing SRR structure is to enhance the antenna in the case of size, gain, directivity, and reflection coefficient.

An impedance matching between tag antenna components could improve the operation power of the chip. So that, it improves the read range.

The performance of the RFID tag antenna design is analyzed through using available full-wave electromagnetic simulator, which is designed on low cost PTFE substrate with dielectric constant of 2.55 (loss tangent 0.001) and thickness equaling 1.5 mm. The compact tag antenna comprises of two split-ring resonator structures mounted to each side of the tag chip. They fed by two symmetrical C-shaped resonators through implementing an inductively coupled feed approach placed on the top surface of PTFE substrate as shown in Figure 3.9.

The proposed antenna changes its resonance frequency by changing the length ( $L_a$ ) and width ( $W_a$ ) of the C-shaped split ring resonator, also the gain of the proposed antenna enhanced when the parameter  $S$  reduced from 0.2 mm to 0.1 mm at the same resonance frequency.

### **3.2.3 Photonic Band Gap Structure**

A photonic band gap (PBG) is a periodic structure that contain a periodic pattern of circles or other shapes in the ground plane of the antenna to prevent the propagation of all electromagnetic waves within a particular frequency band called the band gap.

The surface waves into substrate of the Microstrip antennas are launched when the dielectric constant of substrate equals to  $\epsilon_r > 1$ . It causes serious problems in the antenna such as: limit bandwidth, reducing antenna gain and efficiency.

Impressive progress in the new and emerging area of PBG engineering in recent years has the potential to provide a simple and effective solution to the problems of surface and leaky waves.

PBG structure has many benefits, such as: improved the antenna efficiency, enhanced antenna gain and it is readily applicable to a wide range of frequencies. It is inexpensive and maintains the planer nature of the antenna [33].

### 3.3 Summary

This chapter introduces the methodology of designing the two tag antennas for metallic objects, one with regular ground plane and the other with photonic band gap structure. Achieving matching between the antenna and IC chip depend on modifying the length and width of antenna.

PBG structures integrated with the main design for increasing the gain through etching a periodic pattern of circles. The parameters affecting the resonance frequency and the reflection coefficient which are also been discussed namely: the antenna length ( $La$ ) and the antenna width ( $Wa$ ).

## **CHAPTER FOUR**

### **SPLIT RING RESONATOR BASED UHF RFID TAG ANTENNAS**

- 4.1 Introduction**
- 4.2 SRR Based Antenna with Regular Ground Plane**
  - 4.2.1 Antenna Structure**
  - 4.2.2 Parametric Study**
  - 4.2.3 Simulation and Measurement Results**
- 4.3 SRR Based Tag Antenna with PBG Ground Plane**
  - 4.3.1 Antenna Structure**
- 4.4 Method to enhance the gain for the proposed antenna**
- 4.5 Summary**

## **CHAPTER FOUR**

### **SPLIT-RING RESONATOR-BASED UHF RFID TAG ANTENNAS**

#### **4.1 Introduction**

This chapter introduces two tag antennas, which are printed split-ring resonator-based antennas with regular ground plane and photonic bandgap ground plane for metallic objects with the aim of improving the antenna gain in order to increase the read range. The simulated and measured expected results are verified that attaining a good conjugate between antenna and IC chip at its operating frequency of passive UHF RFID tags. Moreover, details of parametric study, simulated and measured results of the proposed designs.

#### **4.2 SRR-Based Antenna with Regular Ground Plane**

##### **4.2.1 Antenna Structure**

The proposed split-ring resonator-based RFID tag antenna as represented in Figure 4.1 is fabricated on low-cost Polytetrafluoroethylene substrate with permittivity of 2.55 (loss tangent 0.001), and thickness equaling 1.5 mm. The compact tag antenna comprises of two split-ring resonator structures mounted to each side of the tag chip, fed by two symmetrical C-shaped resonators with outer strip lines through implementing an inductively coupled feed approach with 0.2 mm coupling distance placed on the top surface of the PTFE substrate.



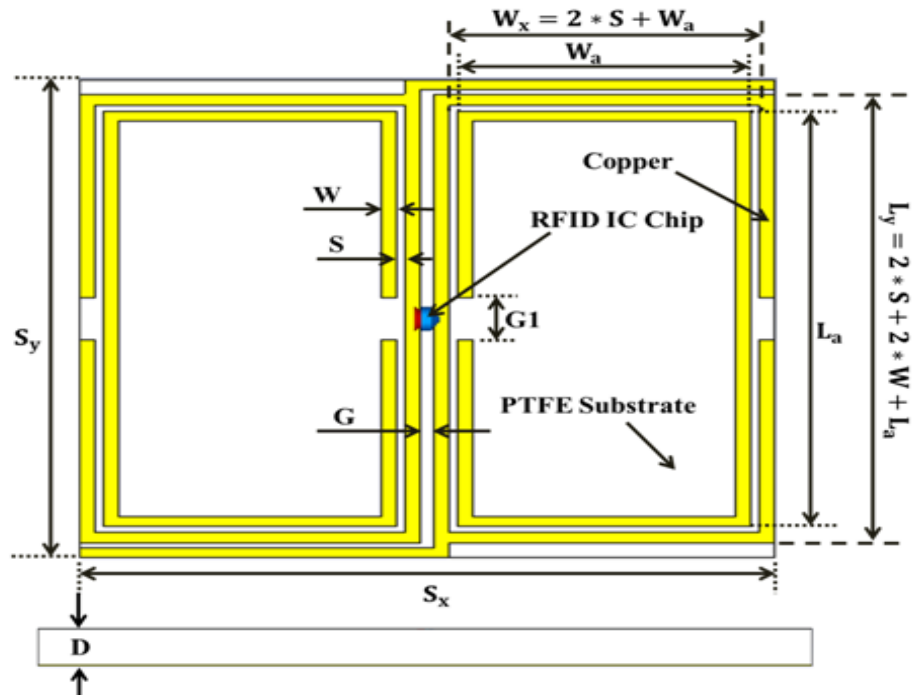


**Figure 4.1.** Geometry of the presented tag antenna,  $S_x=84.5$ ,  $S_y=61.8$ ,  $D=1.57$ ,  $W=0.5$ ,  $S=0.2$ ,  $G=0.5$ ,  $G1=2$ ,  $L_a=59$ ,  $W_a=40.6$  (unit: mm).

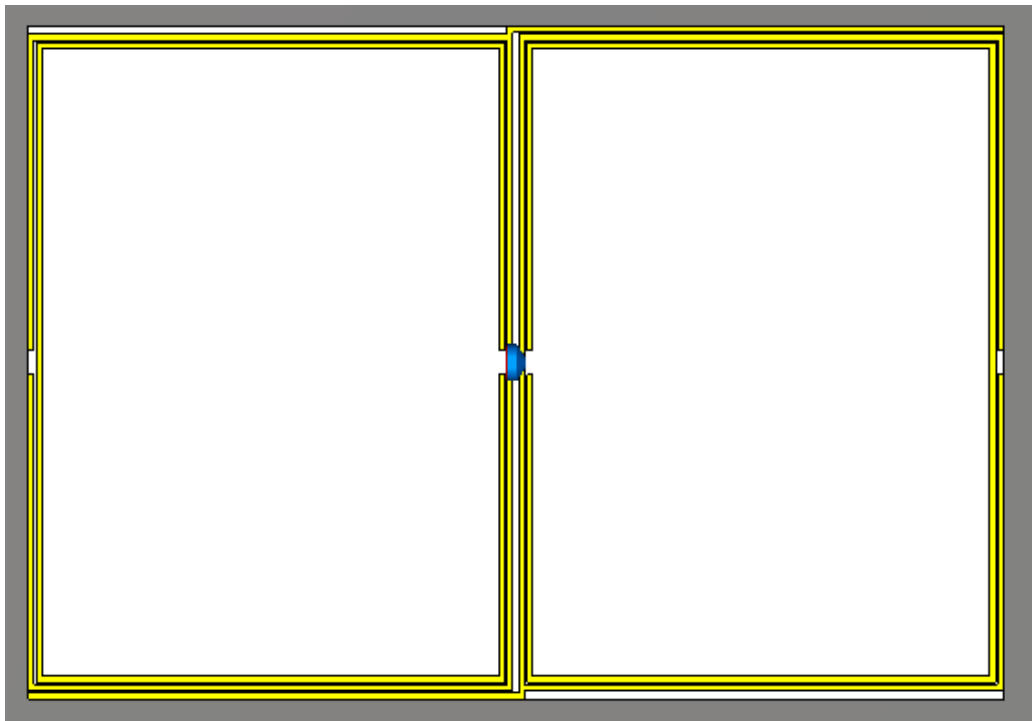


**Figure 4.2.** Geometry of the presented tag antenna on CST program.

The terminals of the IC chip are connected directly to the midpoint of the symmetrical C-shaped resonators by adding the outer strip lines. Meantime the performance of reflection coefficient will enhance by attaining a conjugate between tag antenna and tag chip. The appropriate figures

of geometrical parameters are obtained by tuning the  $L_a$  and  $W_a$  of SRR structure from optimizing simulation to get the best quality for the design at its operating frequency.

#### 4.2.2 Parametric Study

The performance of the RFID tag antenna design such as reflection coefficient, input impedance, read range and the gain of the tag antenna was analyzed through using CST, these performance were tuned by placing the RFID tag antenna on a square perfect electrical conductor (PEC) of 200 mm side length, tag chip of kind Murata RFIDMAGICSTRAP LXMS31ACNA-011 used in the project. The input resistance and reactance of the IC chip is usually designed with low real part and high imaginary part ( $25-j200 \Omega$ ) at its operating frequency 915 MHz.

The length and width of SRR tag antenna are the most parameters that have large effect on the resonance frequency and on the reflection coefficient as exhibited in Table 4.1. The simulation results show that the main factor used to keep the design operating at the RFID standards is by tuning  $L_a$  and  $W_a$ . These parameters are also used to enhance the performance of reflection coefficient.

**Table 4.1.** Simulated results of various values of  $L_a$  and  $W_a$ .

Attempt Number	$L_a$ (mm)	$W_a$ (mm)	reflection coefficient (dB)	resonance frequency(GHz)
1	56	40.2	- 20.764	0.941
2	58	40.2	- 20.728	0.928
3	58	41.2	- 21.27	0.915
4	58	41.4	- 18.987	0.913
5	59	40.6	- 24.312	0.917
6	59	40.8	- 19.44	0.915
7	59	41	- 27.692	0.912
8	60	40	- 23.983	0.919
9	60	40.2	- 32.946	0.916
10	60	40.4	- 19.766	0.913
11	61	40	-21.914	0.913
12	61	40.4	-19.5	0.907

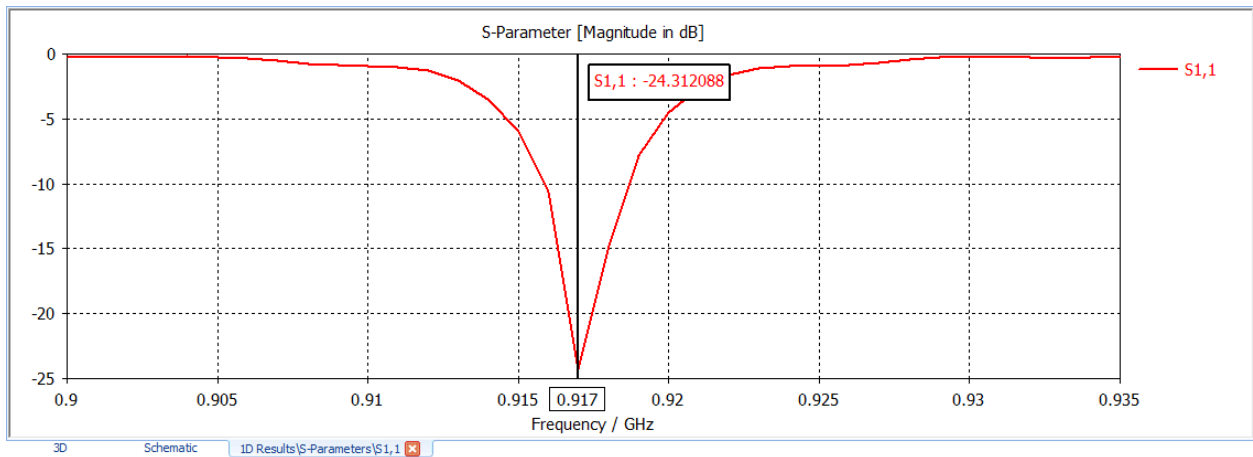


**Figure 4.3.** Simulated reflection coefficient with  $L_a = 59$  (mm) and  $W_a = 40.6$  (mm).

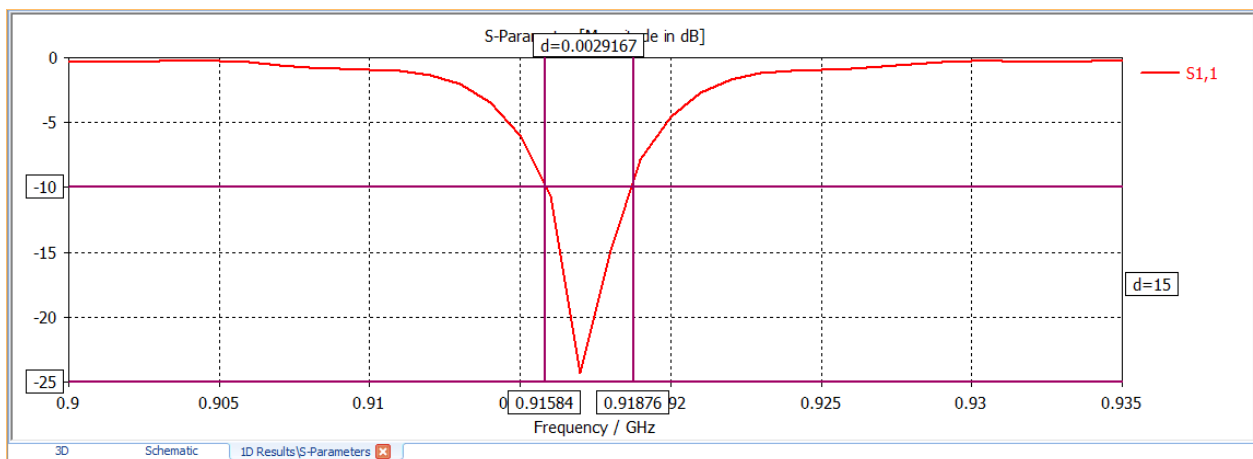


**Figure 4.4.** Simulated bandwidth with  $L_a = 59$  (mm) and  $W_a = 40.6$  (mm).

### 4.2.3 Simulation and Measurement Results

The measurement is performed using the Differential Probe Method, which connects to a 37347D network analyzer from the first side and is soldered to the fabricated design from the second side.

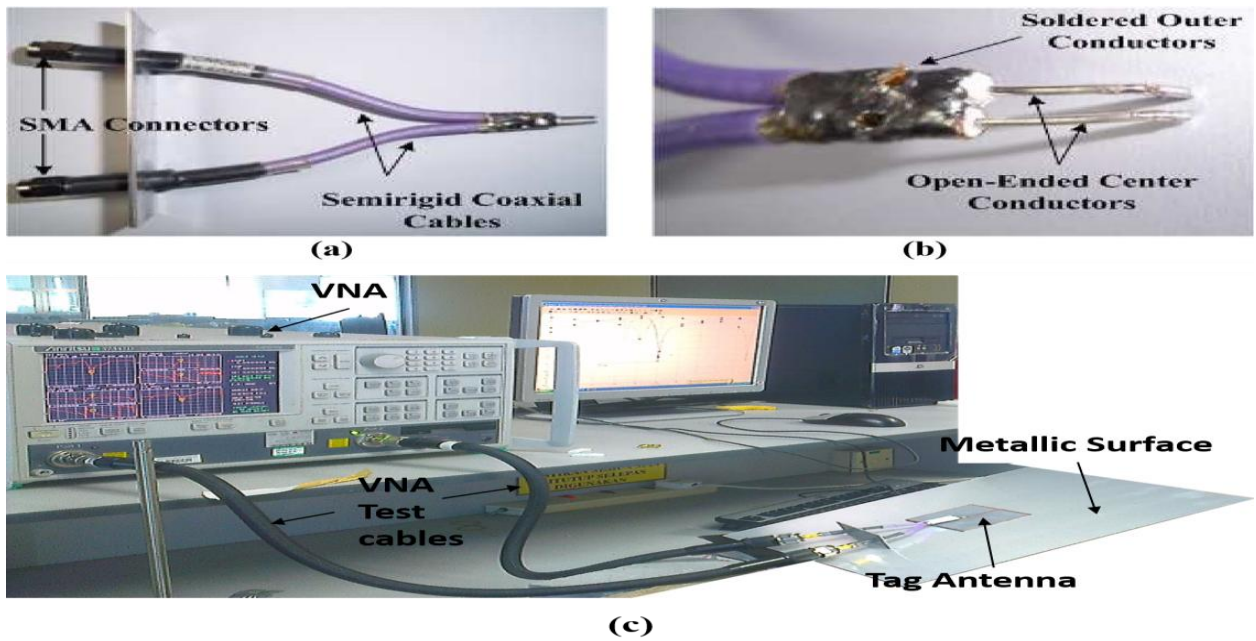


**Figure 4.5.**(a) Semirigid coaxial cables (b) Open ended center conductor of semirigid coaxial cables (c) Examination the antenna using VNA.

A metallic plane can be used to enhance the antenna performance slightly by increasing the size of the metallic surface. Figure 4.6 and Figure 4.7 shows the far-field gain at different sizes of metal plate.

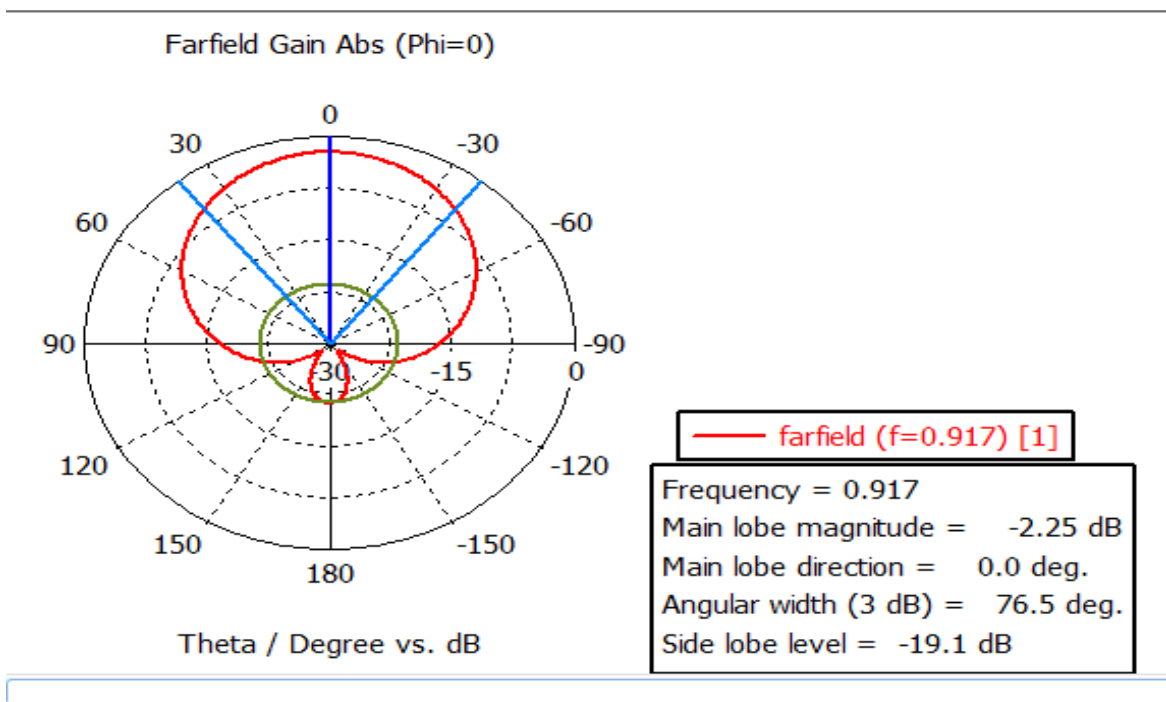


**Figure 4.6.** Simulated far-field radiation pattern at 917 MHz for designed tag antenna with regular ground plane mounted on 200×200 mm<sup>2</sup> metal plate.

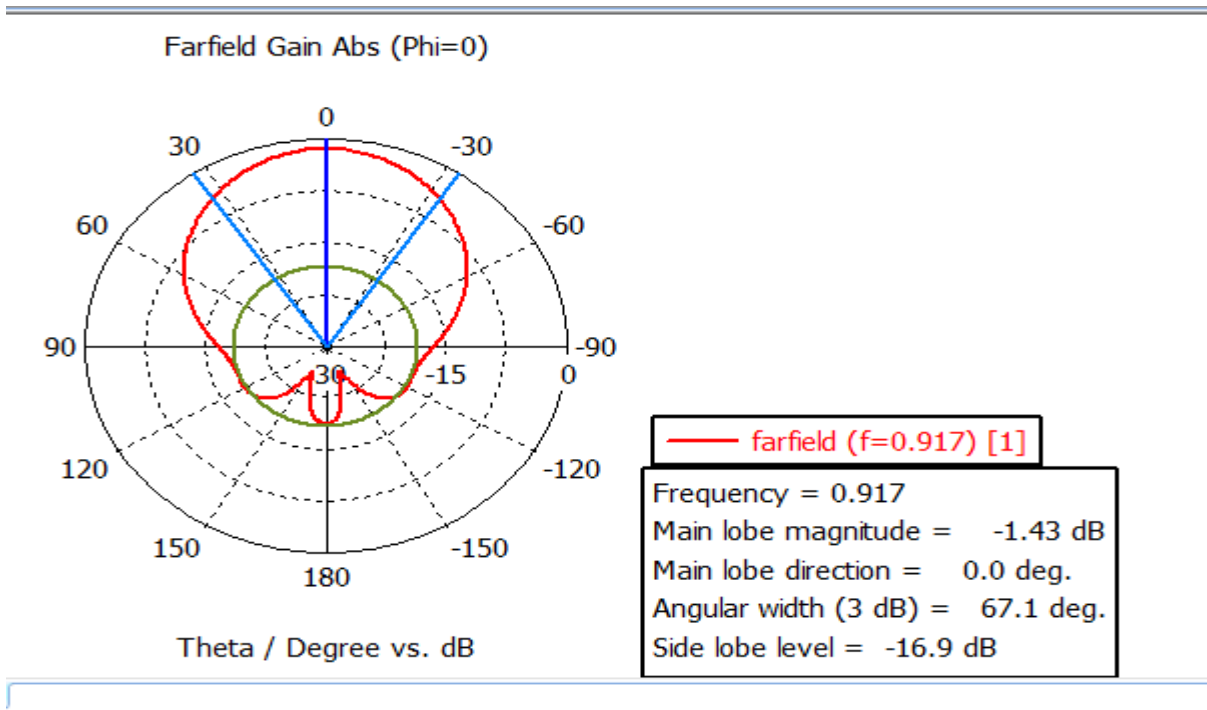


**Figure 4.7.** Simulated far-field radiation pattern at 917 MHz for designed tag antenna with regular ground plane mounted on 400×400 mm<sup>2</sup> metal plate.

Figure 4.8 represents the simulated gain for different metal plates of various sizes. Which clearly obtained that the gain performance enhanced when the ground surface size increased above 200×200 mm<sup>2</sup>.

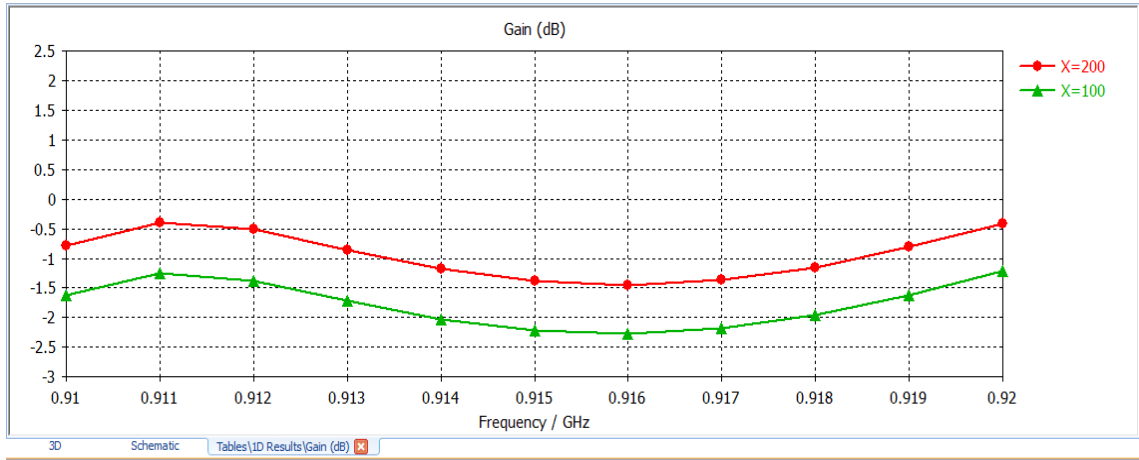


**Figure 4.8.** Simulated gain of the proposed design with regular ground plane placed on various metal plate sizes.

**Table 4.2.** Theoretical maximum read range of the proposed design with regular ground plane.

Condition	Simulated Maximum Gain (dB) @ 917 MHz	Calculated Reading Range (m)
200×200 mm <sup>2</sup> metal plate	-2.25	0.51
400×400 mm <sup>2</sup> metal plate	-1.43	0.56

The maximum theoretical read range is calculated using equation 2.12 which called Friis free space formula as:

$$r = \frac{\lambda}{4\pi} \sqrt{\frac{P_t G_t G_r}{P_{th}}}$$

Where:

$P_t$  is the transmitter (reader) power = 20 dBm = 0.1 W.

$G_t$  is the transmitter (reader) gain = 0.1 dB = 1.0233.

$G_r$  is the design tag antenna gain.

$P_{th}$  is the power threshold of the chip = - 8 dBm = 0.00015849 W.

$\lambda$  is the antenna wavelength.

$$\frac{\lambda}{4\pi} = 0.026037748 \text{ (m)}.$$

The proposed antenna feature a lower read range because of the high threshold power required to turn on the MURATA chip ( - 8 dBm ), the read range can be improved depending on the chip that is used.

The channel capacity of SRR based tag antenna with regular ground plane can be calculated using equation 2.14, 2.15, and 2.16 which are explained in chapter 2 section 2.5.7. Table 4.3 shows the channel capacity and SNR of the system using regular ground plane.

As shown in figure 4.3 the bandwidth of the system is  $918.76 - 915.84 = 2.92$  MHz.

The ideal channel capacity can be calculated using Nyquist capacity formula ( equation 2.14 ) that assumes no noise, by assuming that the system used 4 – Level ASK

$$C = 2W \log_2 M = 2 (2.92 * 10^6) \log_2 4 = 11.68 \text{ Mbps}$$

In practice, the actual bit error rate is always non zero. So the system is exhibited noise, the channel capacity in this case can be calculated using Shannon capacity formula ( equation 2.15 ) and equation 2.16 is also used to calculate the signal to noise ratio (SNR).

Table 4.3 calculated the channel capacity in the case that assumes noise with  $BER = 10^{-6}$  and the corresponding  $\frac{E_b}{N_o}$  equal to 14.5 dB in the case of 4 – Level ASK.

**Table 4.3.** channel capacity of various data rate in the case of assuming noise.

<b>Data Rate (Mbps)</b>	<b>SNR</b>	<b>Channel capacity (Mbps)</b>
<b>0.064</b>	<b>0.6177</b>	<b>2.026</b>
<b>0.320</b>	<b>3.0886</b>	<b>5.93</b>
<b>0.640</b>	<b>6.177</b>	<b>8.30</b>
<b>0.960</b>	<b>9.266</b>	<b>9.811</b>
<b>1.28</b>	<b>12.355</b>	<b>10.918</b>
<b>1.6</b>	<b>15.44</b>	<b>11.79</b>

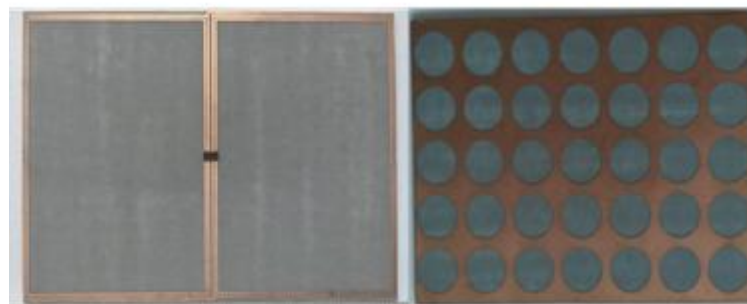
## 4.3 SRR-Based Tag Antenna with PBG Ground Plane

### 4.3.1 Antenna Structure

Through etching a periodic pattern of circles in the ground plane of tag antenna can be formed a simple PBG structure. Various values of the circular slots diameter and the dimension between the circles slots shows the effect of these parameters on the operating frequency and the gain of the design as shown in Table 4.4. The simulation shows that using PBG effect on the resonance frequency but there is no noticeable effect on the gain. So using a periodic of pattern circles to form PBG has no noticeable benefit in this project, maybe different forms rather than circles in the ground of the tag antenna may be useful to enhance the gain.

**Table 4.4.** Simulated results of various values of circular slot diameter and dimension between two circular slots when  $L_a = 59$  (mm) and  $W_a = 40.6$  (mm).

Attempt Number	Circular Slot Diameter R (mm)	Dimension between two circular slots D (mm)	Operating Frequency (GHz)	Gain (dB)
1	3	0.2	0.918	- 2.27
2	4	0.2	0.917	- 2.27
3	5	0.2	0.916	- 2.27
4	5	0.8	0.917	- 2.26
5	5	1	0.918	- 2.24
6	5	1.5	0.919	- 2.25
7	5	2	0.916	- 2.24
8	5	2.2	0.941	----
9	5	2.5	0.922	- 2.44



(a)

(b)

**Figure 4.9.** (a) The designed antenna (b) Backside of PBG design.



**Table 4.5.** Simulated gain for the two desgin @ 917MHz.

Condition	Simulated maximum gain (dB) @ 917 MHz with regular ground plane	Simulated maximum gain (dB) @ 917 MHz with photonic bandgap ground plane
200×200 mm <sup>2</sup> metal plate	- 2.25	- 2.27
400×400 mm <sup>2</sup> metal plate	- 1.43	- 1.44

#### 4.4 Method to enhance the gain for the proposed antenna

As seen in table 4.2 the SRR based tag antenna with regular ground plane has a low value of gain. This gain is achieved when  $L_a = 59$  (mm),  $W_a = 40.6$  (mm) and  $S = 0.2$  (mm). where the parameter S is represented in Figure 3.2 .

After many simulation of various values of parameter S it seems that the gain of the regular ground plane is improved by reducing the value of S from 0.2 to 0.1. Table 4.6 shows the operating frequency and gain of various values of the parameter S. Figure 4.15 exhibit the value of the parameters that used to improve the gain of the regular ground plane

**Table 4.6.** Simulated gain and resonance frequencies for various values of parameter S on 200×200 mm<sup>2</sup>metallic plate.

Attempt Number	The value of the parameter S (mm)	Resonance Frequency (GHz)	Gain (dB)
<b>1</b>	<b>0.10</b>	<b>0.917</b>	<b>- 0.797</b>
<b>2</b>	<b>0.12</b>	<b>0.916</b>	<b>- 0.808</b>
<b>3</b>	<b>0.14</b>	<b>0.915</b>	<b>- 0.813</b>
<b>4</b>	<b>0.15</b>	<b>0.915</b>	<b>- 0.778</b>
<b>5</b>	<b>0.16</b>	<b>0.914</b>	<b>- 0.813</b>
<b>6</b>	<b>0.18</b>	<b>0.918</b>	<b>- 2.40</b>
<b>7</b>	<b>0.20</b>	<b>0.917</b>	<b>- 2.25</b>

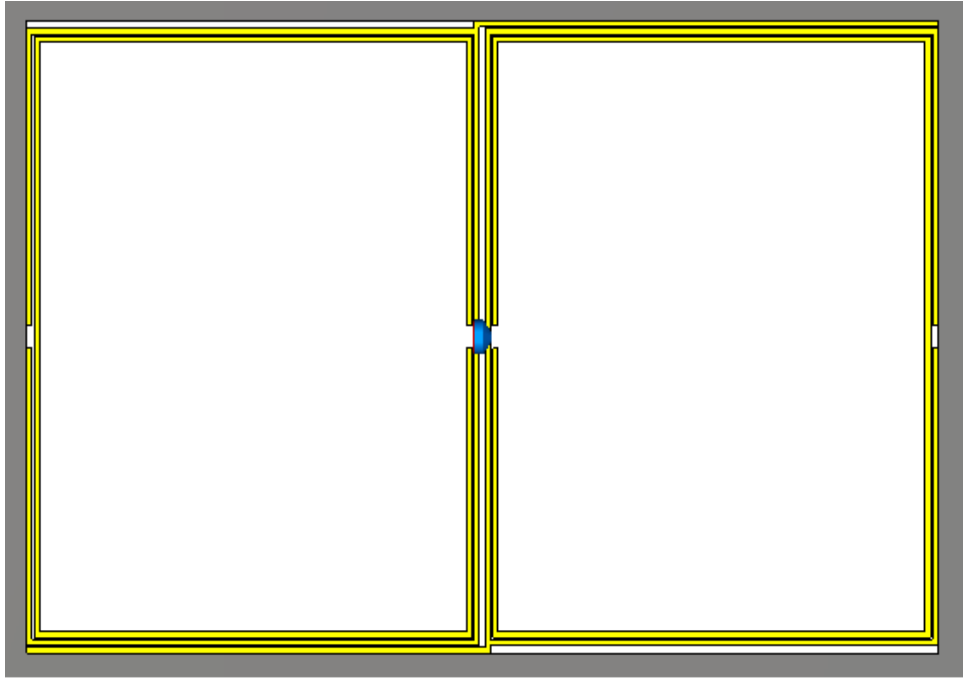


**Figure 4.10.** improved gain of regular ground plane ,  $S_y=61.8$ ,  $S_x=84.5$ ,  $D=1.57$ ,  $W=0.5$ ,  $S=0.1$ ,  $G=0.5$ ,  $G1=2$ ,  $La=59$ ,  $Wa=40.6$  (unit: mm).

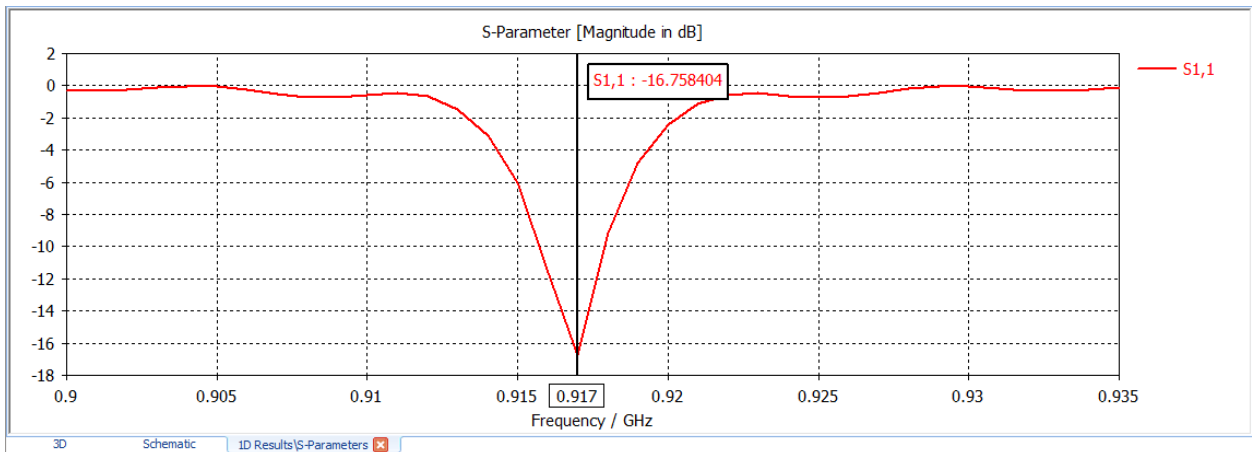


**Figure 4.11.** Simulated reflection coefficient with  $La= 59$  (mm),  $Wa= 40.6$  (mm) and  $S= 0.1$  (mm).

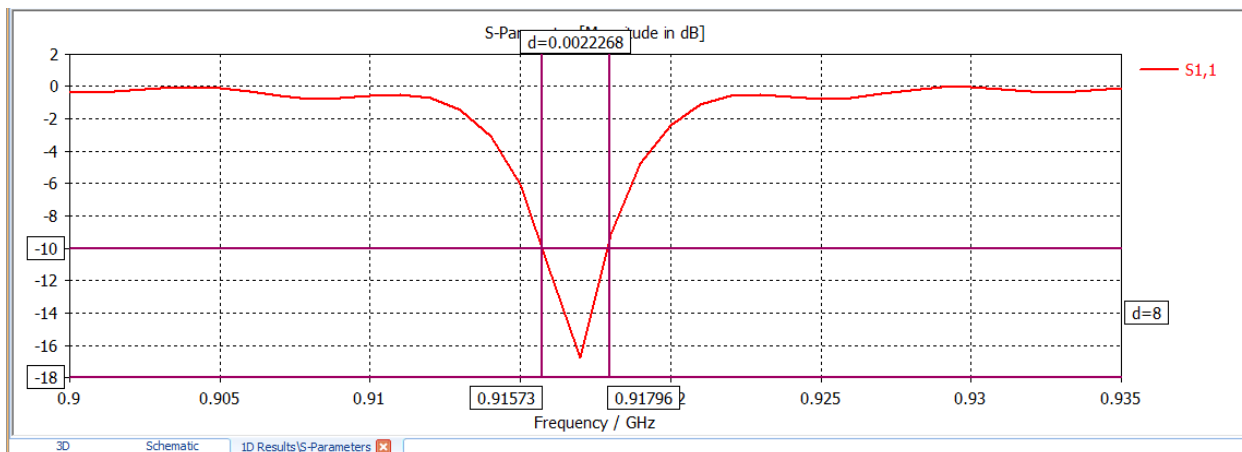


Figure 4.12. Simulated bandwidth with  $L_a = 59$  (mm),  $W_a = 40.6$  (mm) and  $S = 0.1$  (mm).

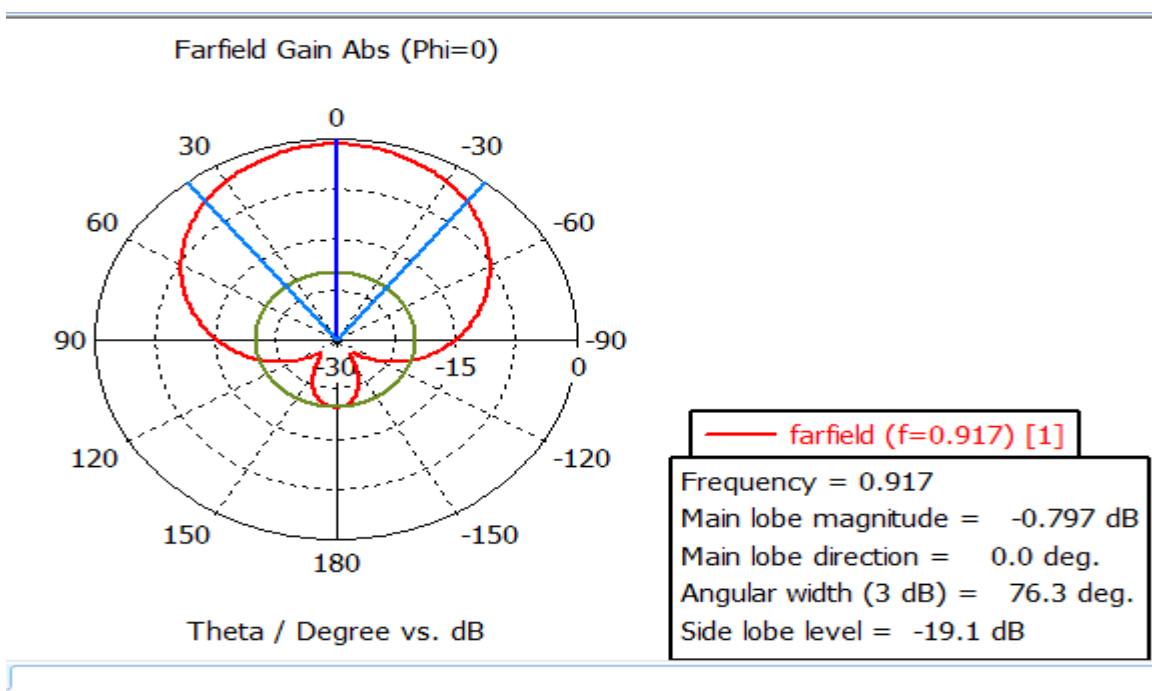
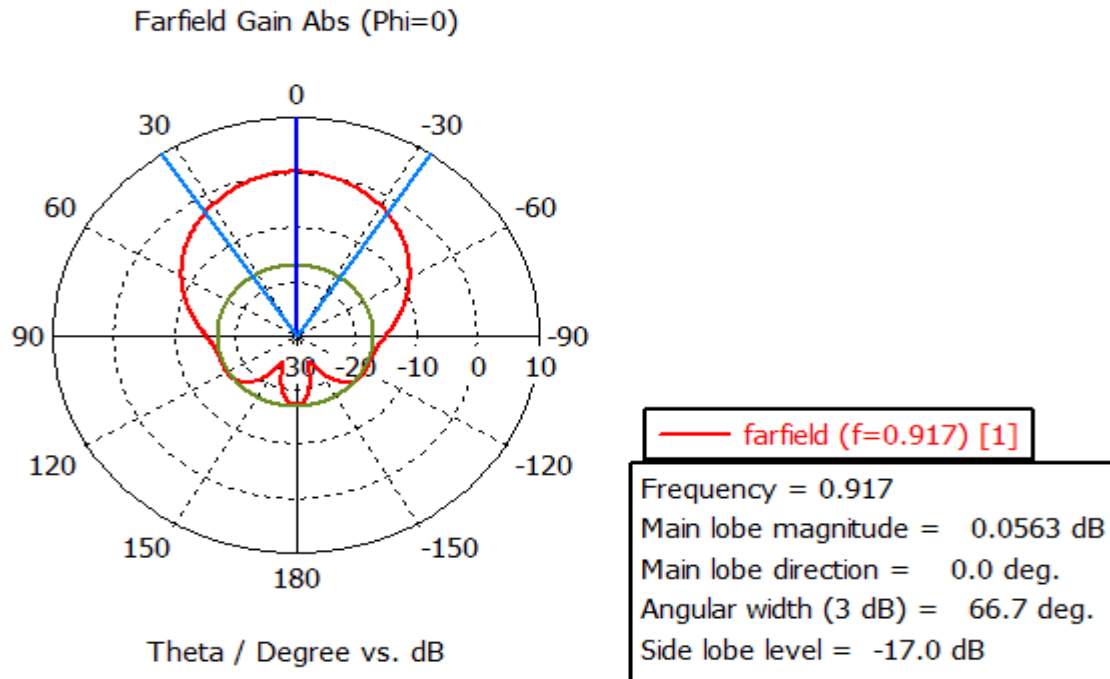


Figure 4.13. Simulated far-field radiation pattern with  $S = 0.10$  (mm) at 917 MHz for designed tag antenna with regular ground plane mounted on  $200 \times 200$  mm<sup>2</sup> metal plate.



**Figure 4.14.** Simulated far-field radiation pattern with  $S = 0.10$  (mm) at 917 MHz for designed tag antenna with regular ground plane mounted on  $400 \times 400 \text{ mm}^2$  metal plate.

**Table 4.7.** Simulated gain for the antenna @ 917 MHz when  $S = 0.10$  mm.

Condition	Simulated Maximum Gain (dB) @ 915 MHz	Calculated Reading Range (m)
200×200 mm <sup>2</sup> metal plate	-0.797	0.6
400×400 mm <sup>2</sup> metal plate	0.0563	0.66

As shown in figure 4.16 the bandwidth of the system is  $917.96 - 915.73 = 2.23$  MHz.

The ideal channel capacity can be calculated using Nyquist capacity formula ( equation 2.14 ) that assumes no noise, by assuming that the system used 4 – Level ASK

$$C = 2W \log_2 M = 2 (2.23 * 10^6) \log_2 4 = 8.92 \text{ Mbps}$$

In practice, the actual bit error rate is always non zero. So the system is exhibited noise, the channel capacity in this case can be calculated using Shannon capacity formula ( equation 2.15 ) and ( equation 2.16 ) is also used to calculate the signal to noise ratio (SNR).

Table 4.8 calculated the channel capacity in the case that assumes noise with  $BER = 10^{-6}$  and the corresponding  $\frac{E_b}{N_o}$  equal to 14.5 dB in the case of 4 – Level ASK.

**Table 4.8.** channel capacity of various data rate in the case of assuming noise with  $S = 0.10$  mm.

<b>Data Rate (Mbps)</b>	<b>SNR</b>	<b>Channel capacity (Mbps)</b>
<b>0.064</b>	<b>0.8088</b>	<b>1.906</b>
<b>0.320</b>	<b>4.044</b>	<b>5.206</b>
<b>0.640</b>	<b>8.088</b>	<b>7.1</b>
<b>0.960</b>	<b>12.133</b>	<b>8.285</b>
<b>1.28</b>	<b>16.177</b>	<b>9.148</b>

**Table 4.9.** Simulated gain for the proposed antennas

<b>Condition</b>	<b>Gain (dB) for SRR based tag antenna with regular ground plane with S = 0.2 @ 917 MHz</b>	<b>Gain (dB) for SRR based tag antenna with regular ground plane with S = 0.1 @ 917 MHz</b>	<b>Percent of Enhancement</b>
200×200 mm <sup>2</sup> metal plate	- 2.25	- 0.797	64.57 %
400×400 mm <sup>2</sup> metal plate	- 1.43	0.0563	103.9 %

Negative gain means that the output is inverted from the input, so if the antenna is radiating in some direction; its directivity is higher than 1 in that specific direction and less than 1 in other non radiating directions.

But for gain, the antenna gain could be any value equal or less than its directivity; depends on the matching and its efficiency, also placing small tag antennas on metallic objects that have higher conductivity and using the metamaterials based antennas that carry large wavelength ( in this project the wavelength is approximately equal to 33 cm ) could be a reason of having negative gain.

**Table 4.10.** percent of reduction of the channel capacity when reducing S from 0.2 mm to 0.1 mm.

<b>Data Rate (Mbps)</b>	<b>Channel capacity (Mbps) of the proposed antenna @ 917 MHz with S = 0.2 mm</b>	<b>Channel capacity (Mbps) of the proposed antenna @ 917 MHz with S = 0.1 mm</b>	<b>Percent of Reduction</b>
0.064	2.026	1.906	5.923 %
0.320	5.93	5.206	12.210 %
0.640	8.30	7.10	14.457 %
0.960	9.811	8.285	15.553 %

The received power of the antenna can be calculated using equation 2.11, table 4.11 shows the received power for the proposed antennas at a distance equal to 0.5 m.

**Table 4.11.** the received power for the proposed antennas @ 0.5 m.

<b>Condition</b>	<b>Gain (dB) for the proposed antenna with S = 0.2 @ 917 MHz</b>	<b>Received power (<math>\mu w</math>) @ 0.5 m for the proposed antenna with S = 0.2 @ 917 MHz</b>	<b>Gain (dB) for the proposed antenna with S = 0.1 @ 917 MHz</b>	<b>Received power (<math>\mu w</math>) @ 0.5 m for the proposed antenna with S = 0.1 @ 917 MHz</b>	<b>Percent of Enhancement of the received power @ 0.5 m</b>
200×200 mm <sup>2</sup> metal plate	- 2.25	161.489	- 0.797	225.654	39.7 %
400×400 mm <sup>2</sup> metal plate	- 1.43	195.049	0.0563	274.646	40.8 %

## 4.5 Summary

Design and simulation of the UHF RFID placed on metallic object is present to be near the resonant frequency, main part for RFID is the antenna. The main core of transmit and receive the information is the antenna. The design and simulation of the antenna is given using CST STUDIO, frequency domain signal are simulated S-parameter and gain in dB.

The project focus on the development of microstrip antenna for RFID tags that placed on a metallic application object which has a size of ( 84.5×61.8×1.57 mm<sup>3</sup>), and placed on PTFE substrate with thickness 1.5 mm . A main task of our investigation will concentrate on studying the range distance and its effect on the design. To improve the read orientation sensitivity, we will consider design tags with SRR as well looking into the effect changing for the size of the metamaterial to minimize the antenna size, improve the gain and enhance the read range.

Reflection coefficient performance is affected through changing the vital parameters  $L_y$  and  $W_x$  C-shaped resonators. The structure of the tag antenna give a flexible method to attain an excellent impedance matching between antenna and IC chip to improve the performance of reflection coefficient, gain and read ranges.

The resonance frequency of the proposed tag antenna shifted when changing the length and width of SRR, also the reflection coefficient, gain, directivity and read range changed.

The accreditation will be on the frequency equal to 917 MHz when the tag antenna placed on regular ground plane, and this frequency achieved when the length and width of SRR equal to 59 mm and 40.6 mm respectively, the best gain and read range achieved was  $-1.43$  dB and 0.56 m respectively when the tag antenna placed on  $400 \times 400$  mm<sup>2</sup> metal plate.

PBG structure is formed by placing any periodic shapes in the ground of the tag antenna, in this project periodic circles were placed in the ground of the tag antenna. After studying the PBG structure by trying different values of the diameters of the circles and the distance between these circles note that the effect be on the resonance frequencies without any improvement on the gain of the antenna, So trying periodic circles to form PBG did not help to improve the gain, may be different shapes rather than circles did that.

Finally, the study of some parameters of the tag antenna especially the S- parameter to try to improve the gain, and it was found that by decreasing the value of S from 0.2 mm to 0.1 mm, the gain and the read range of the tag antenna enhanced from  $-1.43$  dB and 0.56 m to 0.0563 dB and 0.66 m respectively when the tag antenna placed on  $400 \times 400$  mm<sup>2</sup> metal plate.



## **CHAPTER FIVE**

### **SUMMARY AND DESIGN APPLICATION**

**5.1 Summary**

**5.2 Design Application**

**5.3 Future Work**

## CHAPTER FIVE

### SUMMARY AND DESIGN APPLICATION

#### 5.1 Summary

Modern RFID tag antenna arranged on metallic objects with high gain, little reflection coefficient, and small size is the most challenging issue. Nowadays, many researchers have used metamaterials to improve the performance of RFID tag antennas. Some recent works on metamaterial inspired antennas have pointed out that the metamaterial based antennas are capable of equally exhibiting similar characteristics seen in large antennas like patch antennas.

Two SRR based tag antenna are presented in chapter four for RFID metallic object applications. One with regular ground plane and the other with photonic bandgap ground plane, Each antenna design was etched on PTFE substrate.

The SRR based antenna with regular ground plane achieved equally gain with SRR based antenna with photonic bandgap plane. The maximum gain and read range of SRR based tag antenna with regular ground plane is - 1.43 dB and 0.56 m respectively when placed on  $400 \times 400 \text{ mm}^2$  metallic plate and the parameter  $S = 0.2 \text{ mm}$ , while the maximum gain and read range of SRR based tag antenna with regular ground is 0.0563 dB and 0.66 m respectively when placed on the same size of metallic plate and the parameter  $S = 0.1 \text{ mm}$ . The read range of the two designs are obtained by using 20 dBm radiation power of the RFID reader.

#### 5.2 Design Application

The proposed split ring resonator tag antennas with regular ground and PBG ground will be designed to operate at UHF frequency band with capability to improve their performance.

The SRR based tag antenna in this project can be applied in several applications such as:

- a) Transportation sector: where the designed antenna can be placed on the car bodies especially in municipal parks in order to alleviate the congestion and to order the internal and external lines of the cars also to ordering the electronic accounting within the car parks, thus to facilitate the daily life in the communities.

- b) Industry and Commerce: the project can be used to import and export metallic materials, food cans, medical devices, and gold.
- c) Petroleum Engineering sector: the project helps to differentiate between the various petroleum products and to know the amount and the date of the products, in addition to knowing the issuers and the importers of the products.

### **5.3 Future Work**

Further work may consider to try applying the proposed design on other metamaterial shape and application rather than metallic application and concentrating to have higher gain and therefore higher read range.

## REFERENCE

- [1] J. Uddin, M. B. I. Reaz, M. Hasan, A. Nordin, M. Ibrahimy, and M. A. M. Ali, "UHF RFID antenna architectures and applications," *Scientific Research and Essays*, vol. 5, pp. 1033-1051, 2010.
- [2] L. Catarinucci, R. Colella, M. D. Blasi, L. Patrono, and L. Tarricone, "Experimental Performance Evaluation of Passive UHF RFID Tags in Electromagnetically Critical Supply Chains," *Journal of Communications Software & Systems*, vol. 7, 2011.
- [3] H. Vogt, "Efficient object identification with passive RFID tags," in *Pervasive computing*, ed: Springer, 2002, pp. 98-113.
- [4] M. A. Aris, E. A. Kadir, M. Y. M. Zain, Z. I. Rizman, and N. H. R. a. Husin, "A Miniature UHF Rectangular Microstrip RFID Tag Antenna for Aluminium Can Application," *World Applied Sciences Journal*, vol. 23, pp. 96-102, 2013.
- [5] S. More and M. Turuk, "Compact microstrip antenna for RFID application," *Progress in International Journal of Emerging Technology and Advanced Engineering*, vol. 2, 2012.
- [6] J. Landt, "The history of RFID," *IEEE potentials*, vol. 24, pp. 8-11, 2005.
- [7] M. Roberti, "The history of RFID technology," *RFID journal*, vol. 16, 2005.
- [8] J. Landt, "Shrouds of Time: The history of RFID, Pittsburgh, AIM-Inc," ed: Mar, 2005.
- [9] U. V. S. B. Alliance, "RFID feasibility study, final report," *Application note*.
- [10] S. A. Weis, "Rfid (radio frequency identification): Principles and applications," *System*, vol. 2, p. 3Principles, 2007.
- [11] A. S. A. Jalal, A. Ismail, A. R. H. Alhawari, M. F. A. Rasid, N. K. Noordin, and M. A. Mahdi, "Miniaturized metal mount Minkowski fractal RFID tag antenna with complementary split ring resonator," *Progress In Electromagnetics Research C*, vol. 39, pp. 25-36, 2013.
- [12] D. W. Engels and S. E. Sarma, "Standardization requirements within the RFID class structure framework," *Auto-ID Labs, Massachusetts Institute of Technology, Cambridge, MA USA, Tech. Rep*, 2005.
- [13] C. A. Balanis, "Fundamental parameters of antennas," *Antenna Theory Analysis and Design*, pp. 27-132, 2005.
- [14] S. Drabowitch, A. Papiernik, H. Griffiths, J. Encinas, and B. L. Smith, *Modern antennas*: Springer Science & Business Media, 2010.
- [15] G. De Vita and G. Iannaccone, "Design criteria for the RF section of UHF and microwave passive RFID transponders," *IEEE transactions on microwave theory and techniques*, vol. 53, pp. 2978-2990, 2005.

- [16] K. S. Rao, P. V. Nikitin, and S. F. Lam, "Antenna design for UHF RFID tags: a review and a practical application," *Antennas and Propagation, IEEE Transactions on*, vol. 53, pp. 3870-3876, 2005.
- [17] K. S. Rao, P. V. Nikitin, and S. F. Lam, "Impedance matching concepts in RFID transponder design," in *Automatic Identification Advanced Technologies, 2005. Fourth IEEE Workshop on*, 2005, pp. 39-42.
- [18] K. Kurokawa, "Power waves and the scattering matrix," *Microwave Theory and Techniques, IEEE Transactions on*, vol. 13, pp. 194-202, 1965.
- [19] P. V. Nikitin, K. S. Rao, S. F. Lam, V. Pillai, R. Martinez, and H. Heinrich, "Power reflection coefficient analysis for complex impedances in RFID tag design," *IEEE Transactions on Microwave Theory and Techniques*, vol. 53, pp. 2721-2725, 2005.
- [20] S. Konya, T. Sasamori, T. Tobana, and Y. Isota, "Wideband impedance measurement of balanced antenna using the S-parameter method," in *Microwave Conference Proceedings (APMC), 2011 Asia-Pacific*, 2011, pp. 717-720.
- [21] S.-K. Kuo, S.-L. Chen, and C.-T. Lin, "An accurate method for impedance measurement of RFID tag antenna," *Progress In Electromagnetics Research*, vol. 83, pp. 93-106, 2008.
- [22] K. D. Palmer and M. W. van Rooyen, "Simple broadband measurements of balanced loads using a network analyzer," *IEEE transactions on instrumentation and measurement*, vol. 55, pp. 266-272, 2006.
- [23] K. D. Palmer and M. W. Van Rooyen, "Simple broadband measurements of balanced loads using a network analyzer," *Instrumentation and Measurement, IEEE Transactions on*, vol. 55, pp. 266-272, 2006.
- [24] G. C. Temes and J. W. Lapatra, *Introduction to circuit synthesis and design*: McGraw-Hill Companies, 1977.
- [25] N. Fang, H. Lee, C. Sun, and X. Zhang, "Sub-diffraction-limited optical imaging with a silver superlens," *Science*, vol. 308, pp. 534-537, 2005.
- [26] M. Olyphant Jr and T. E. Nowicki, "Microwave substrates support MIC technology. I," *Microwaves*, vol. 19, pp. 74-76, 1980.
- [27] G. Traut, "Clad laminates of PTFE composites for microwave antennas," *Microwave journal*, vol. 23, pp. 47-51, 1980.
- [28] R. W. Ziolkowski and C.-C. Lin, "Metamaterial-inspired magnetic-based UHF and VHF antennas," in *Antennas and Propagation Society International Symposium, 2008. AP-S 2008. IEEE*, 2008, pp. 1-4.
- [29] S. Naoui, L. Latrach, and A. Gharsallah, "Equivalent Circuit Model for Double Split Ring Resonators," *INTERNATIONAL JOURNAL*, vol. 11, p. 1, 2016.

- [30] M. Wu, F. Meng, Q. Wu, J. Wu, and L. Li, "A compact equivalent circuit model for the SRR structure in metamaterials," in *Microwave Conference Proceedings, 2005. APMC 2005. Asia-Pacific Conference Proceedings, 2005*, p. 4 pp.
- [31] S.-H. Lim, Y.-C. Oh, H. Lim, Y.-S. Lee, and N.-H. Myung, "Analysis and design of a UHF RFID tag antenna with a split ring resonator," in *Antenna Technology: Small Antennas and Novel Metamaterials, 2008. iWAT 2008. International Workshop on, 2008*, pp. 446-449.
- [32] F. N. Erman, A. Ismail, R. S. A. R. Abudullah, A. R. H. Alhawari, and A. A. Shabaneh, "UHF RFID split-ring resonator tag antenna inductively coupled feed for metallic object," in *2015 IEEE 12th Malaysia International Conference on Communications (MICC), 2015*, pp. 74-76.
- [33] B. Gao and M. M. Yuen, "Passive UHF RFID packaging with electromagnetic band gap (EBG) material for metallic objects tracking," *IEEE Transactions on Components, Packaging and Manufacturing Technology*, vol. 1, pp. 1140-1146, 2011.